Univerzita Karlova v Praze

Přírodovědecká fakulta

Ústav hydrogeologie, inženýrské geologie a užité geofyziky

Studijní program: Geologie

Studijní obor: Geologie

Václav Kuna

Subdukční továrna: interakce magmatu s nadložním litosférickým klínem

Subduction factory: interaction of subduction-related magma with the overlying lithospheric wedge.

BAKALÁŘSKÁ PRÁCE

Vedoucí závěrečné práce: RNDr. Aleš Špičák CSc.

Praha, 2011

Prohlašuji, že jsem závěrečnou práci zpracoval samostatně a že jsem uvedl všechny použité informační zdroje a literaturu. Tato práce ani její podstatná část nebyla předložena k získání jiného nebo stejného akademického titulu.

V Praze, 22.8.2011 Václav Kuna

Poděkování

Rád bych poděkoval všem, kdo se podíleli na vzniku mé bakalářské práce. Zejména chci poděkovat vedoucímu práce RNDr. Aleši Špičákovi CSc. a konzultantu RNDr. Jiřímu Vaňkovi DrSc. za námět práce, nesčetné korektury a trpělivost. Děkuji taktéž všem členům oddělení Tektoniky a geodynamiky za vytvoření přátelského prostředí a rodičům za neustálou podporu mých studií.

Contents

1. Introduction **1**

2. Basic principles **2**

2.1. Volcanism at convergent plate margins 2

2.1.1. Volcanic chains at convergent plate margin 2

2.1.2. Magma melting 2

2.1.3. Geologic environment of the arc area 3

2.1.4. Geochemical characteristic of arc volcanic rocks 3

2.1.5. Extensional vs. Compressional arcs 5

2.2. The seismological background 6

2.2.1. Earthquake parameters 7

2.2.2. Focal mechanisms 8

2.2.3. Seismic sequences 9

2.2.4. Wadati-Benioff zone and its specific features 10

3. The interaction of magma with the overlying mantle wedge **11**

3.1. Introduction 11

3.2. Area of interest 12

3.3. Data 12

3.3.1. EHB database 12

3.3.2. Global centroid moment tensor solution 16

3.3.3. Other data used 16

3.4. Method 16

3.4.1. Searching for earthquake sequences 17

3.5. Volcanic domains 17

3.5.1. Domain 1 17

3.5.2. Domain 2 21

3.5.3. Domain 3 25

3.5.4. Domain 4 29

3.5.5. Domain 5 31

4. Conclusions **36**

References **38**

1. Introduction

The world's largest earthquakes, the most destructive tsunamis and the most explosive volcanism are generated at subduction zones at convergent plate margins. These are often areas with high population density where plenty of mineral resources have been accumulated over geologic time. Despite of high societal and economic importance of these areas, there are still some poorly understood processes and unresolved problems, such as the process of magma generation and ascent to the Earth surface. Recently, attention of many research groups around the world is given to the investigation of convergent plate margins e.g. the National Oceanic and Atmospheric Administration (NOAA) projects, International Continental Drilling Program (ICDP) projects or projects of Japanese geoscientists at Institute of Research on Earth Evolution (IFREE), Japan Agency for Marine-Earth Science and Technology (JAMSTEC). However, the development of these research projects is hindered by the complexity and inaccessibility of the studied processes. The plate tectonics group of the Institute of Geophysics of the Academy of Sciences of the Czech Republic (IG AS CR) has been exploring the above-mentioned processes for a considerable time. The following phenomena were studied in particular: disastrous earthquakes (e.g. Vaněk et al., 2000; Špičák et al., 2007b), seismo-volcanic interactions (e.g. Špičák et al., 2005, 2008) and accumulation of metals (e.g. Hanuš et al., 2000). The attention has been concentrated to four convergent margins: Andean South America, Central America, Western Pacific and Southeast Asia.

This study continues in the investigation of the interaction of the subduction-related magma with the overlying lithospheric wedge above the subduction zone, which has been studied by the plate tectonics group of the IG AS CR (Špičák et al., 2004, 2005). The present study consists of two parts: in the first one, the phenomenon of volcanism at convergent plate margins and seismological backgroung are described, while the second part explores the earthquake occurrence beneath volcanoes in the broader region of the Banda Arc (Indonesia).

2. Basic principles

2.1. Volcanism at convergent plate margins

2.1.1. Volcanic chains at convergent plate margin: Island arc, Continental margin arc

Magmatism at convergent plate boundaries is mostly represented by a linear or curved chain of volcanoes, called volcanic arc, which is typically positioned parallel to the plate margin and expressed morphologically by a deep trench at the sea floor. The arc can be placed either on oceanic or continental lithosphere. In the first case, the volcano has to produce a considerable volume of magma to reach the water level. If this occurs, the volcanic arc is called island arc. This type is represented e.g. by several arcs in the western Pacific: Aleutians, Kuriles, Izu-Bonins, Marianas, New Hebrides and Tonga-Kermadec. These regions are known as supra subduction zones (SSZ) (Sigurdsson et al., 2000), which means that tectonic processes here are very active; magma erupts to forearc, arc and backarc and sediments are metamorphosed and accreted to the arc. After a sufficiently large volume of magmatic, sedimentary and metamorphic material has accumulated to the island arcs, an extensive land underlain by young crust can be created, which is placed between the original island arc built on the oceanic lithosphere and the continental margin arc built on the old continental plate basement. This character embodies for example New Zealand, Japan, Kamchatka, the Cascades and Java. The South American Andes are the second type of arcs grown on continental lithosphere which consists of subaerial volcanoes (Sigurdsson et al., 2000).

The volcanic chain is often segmented, which reflects the tectonic structure of both the subducted slab and overlying plate e.g. by presence of transform faults.

2.1.2. Magma melting

According to Sigurdsson (Sigurdsson et al., 2000) magma is generated within the mantle wedge above the subducting slab. The mantle melting is thought to be an effect of hydration of the mantle by volatiles released from the subducted slab into the overlying mantle

wedge, which implicates lowering of the temperature of solidus of the wedge. This corresponds to thermal models of subduction zones, which assume that the temperature in depths from 100 to 150 km is below the solidus in the subucted slab. There is a significant relation between the positions of volcanic arc (distance from the trench to the arc) and the depth of the Wadati-Benioff zone beneath the volcanic arc; in other words the distance trench – arc depends on the subduction dip. That means that the trigger of magmatic processes is pressure dependent. This suggestion is further supported by the fact that when penetration of the subducting slab stops (it is not moving deeper in the mantle), there is no active volcanism at the surface. This is explained as a lack of volatiles at depths from 100 to 150 km where temperature of the mantle wedge is close to its solidus and volatiles would cause melting of the mantle. (Sigurdsson et al., 2000). This theory is not supported by observations of Špičák et al. (2004, 2005) who considered that the magma source area could be placed within the subducting slab. This hypotheses arised from the fact that the mantle wedge is – in contrary to the subducting slab – capable of brittle failure and therefore is probably not melted.

2.1.3. Geologic environment of the arc area

Subaerial arcs consist of magma flows and pyroclastic rocks often occurring in large stratovolcanoes. Eruptions are commonly of Plinian character producing much of the ejecta in the form of ash and dust. Explosivity of eruptions grows generally with growing content of felsic minerals and fluids in magma. Submarine arcs are represented by pillowed basalt flows and large volumes of hyaloclastic tuffs and breccias (Condie, 1997).

2.1.4. Geochemical characteristic of arc volcanic rocks

The most common rock type at volcanic arcs is andesite with the intermediate content of SiO_2 (Fig. 1. (a)). The occurrence of basaltic and rhyolitic rocks is sparse and depends on the rate of fractional crystallization of the ascending magma. Basalts can occur at oceanic arcs, dacites at continental-margin arcs. The rocks from the volcanic arcs are of calc-alkaline character with relatively high content of calcium (CaO), potassium (K_2O) and sodium (Na_2O) and depleted in magnesium (MgO) and iron (FeO). The rate FeO/MgO grows slightly with increasing percentage of SiO_2. These rocks are distinct from other basaltic volcanic rocks at midocean ridges that are of tholeitic character (poor in sodium and

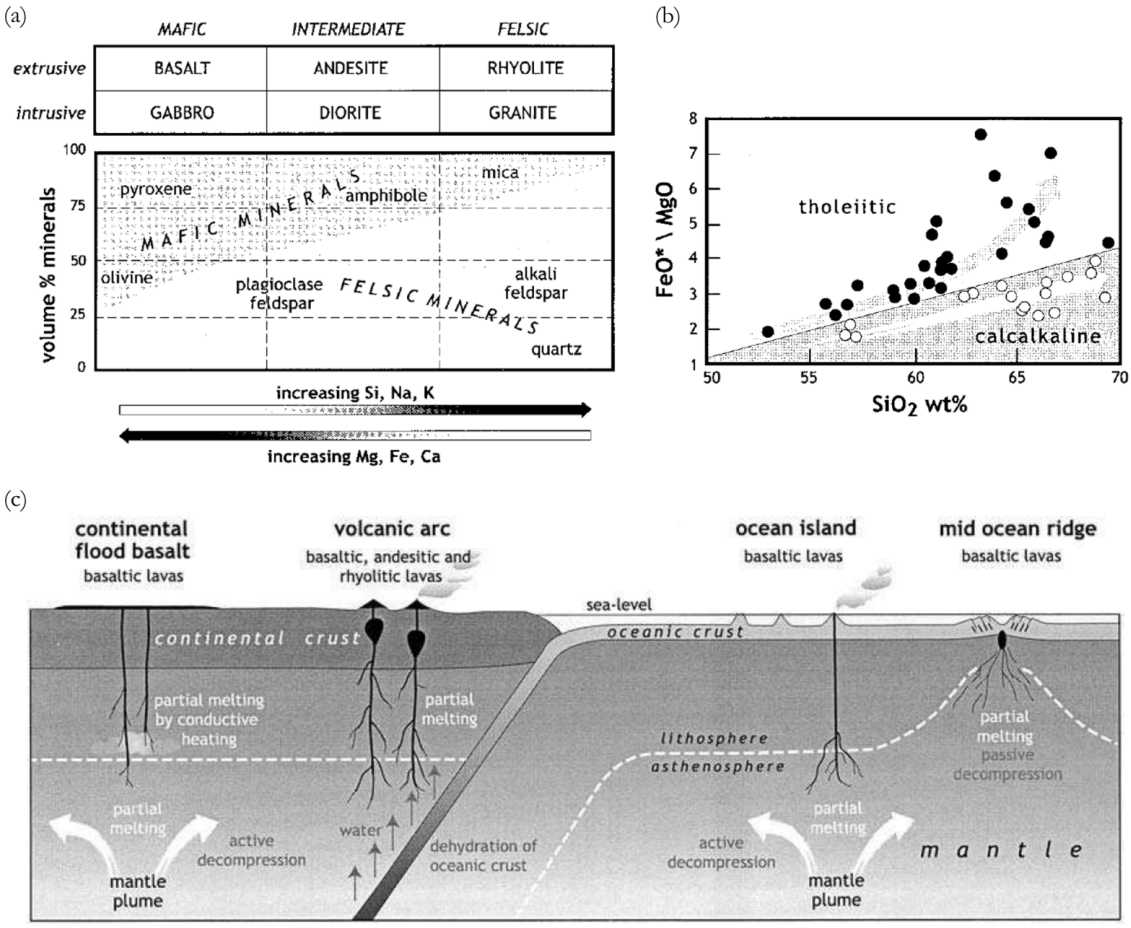

Fig. 1. (a) The mineralogy and the general compositional characteristics of the most common igneous rock types. (b) Contrasting FeO/MgO ratios in calcalkaline and tholeiitic rocks from Aso, a Japanese volcano. Fractionation of olivine and plagioclase in the tholeiitic suite produces iron enrichment and hence high FeO/MgO ratios for a given increase in SiO2, whereas early fractionation of clinopyroxene and olivine in the calcalkaline trend produces less iron enrichment and a more rapid increase in SiO2 . (c) A diagrammatic section through the continent and ocean showing crust and mantle lithosphere and melting mechanisms for MORB, OIB, island arcs, and continental flood basalts. (Sigurdsson et al., 2000)

potassium) with rapidly growing rate FeO/MgO for a given increase in SiO_2 (Fig. 1. (b); (c)).

2.1.4.1. Specific types of rocks at volcanic arcs

In an early stage of magmatism (close to the trench) – it means at depths where the slab is shallower than 100 km – rocks called boninite occur. They have high magnesium, high silica content, with very low volumes of fluid mobile incompatible trace elements. With increasing depth of the subducting slab the content of mobile incompatible elements is increasing. This trend is expressed as „K-h relationship", which means that with increasing depth of the Wadati-Benioff zone the portion of potassium in lava increases. This hypothesis supports the fact that at some well-developed trenches, back-arc volcanism with high potassium alkaline lava (product called shoshonite) occurs. Provided that the rate of partial melting is dependent on the amount of volatiles released from the subducted slab into the overlying mantle wedge and the content of volatiles is with increasing depth of the subducting slab getting lower, the rate of partial melting with increasing depth of subduction is lower. So the probable cause of this trend is that the content of potassium is dependent on the rate of partial melting of magma (Sigurdsson et al., 2000).

There are several subduction zones where the subducted slab reaches abnormally high temperatures. This seems to be the consequence of low age of the subducting slab. Rocks from the source like this differ from those at the other arcs by higher content of SiO_2 and lower content of K and are known as adakites (Sigurdsson et al., 2000).

2.1.5. Extensional vs. Compressional arcs

The state of stress at a convergent margin is controlled by the relative velocity of movement of both the subducting slab and the overlying plate. Sinking of oceanic lithosphere is driven by the density difference between the lithosphere and the underlying mantle. The density of the oceanic lithosphere is largely controlled by its age. When the lithosphere is formed at a spreading center, it is hot, thin and therefore buoyant, but when it moves from the divergent margin it becomes colder and thicker, so the density grows. In case that the slab sinks rapidly, it sweeps into the mantle like a paddle, subsiding at a steeper angle and causing the hinge line to migrate away from the arc in a process known as a slab rollback. Despite the relative movement of both plates, there is continuous contact between these two plates. The upper plate is pulled by the subducting lithosphere, which leads to a pro-

cess called backarc spreading. If the lithosphere that comes to the margin is younger and more buoyant, the effect is to impede the subduction. The angle of the subduction decreases, which leads to greater area in contact with more viscous overlying lithosphere. This causes compressional stresses which are transmitted into the upper plate and may lead to deformation such as folding and thrust faulting in the crust. The relative velocity of the upper plate is also important for the angle of subduction – higher velocity leads to shallowing of subduction.

The different architecture of a convergent margin led to definition of two end member types of behavior. Mariana type, common in the western Pacific, is characterized by steep subduction of old dense slab with extensional regime and development of backarc basins. The Chilean type is represented by gentle subduction of buoyant slab commonly accompanied by compression. Generally there is no backarc extension there (Sigurdsson et al., 2000).

2.2. The seismological background

An earthquake is a result of a sudden release of energy in the form of seismic waves. Earthquakes are almost always related to faults – internal surfaces in the Earth where one side moves with respect to the other. The near surface earthquakes usually occur at known faults (which were earlier identified e.g. by geological mapping) that points to a fact that motion along the fault has already occurred in the past. Sudden earthquake occurrence is explained by the elastic rebound theory. According to this theory the blocks on both sides of the fault move in respect to each other, but friction "holds" the fault confined and prevents movement. When the strain accumulated in the medium reaches a boundary value, the fault slips and releases energy in form of seismic waves (Stein, 2003). This behavior is called brittle-elastic and rocks behave this way at low temperatures and high strain rates (Park, 1983). Primarily they deform elastically; when the stress grows up to about 70% of their strength, the brittle behavior becomes dominant. The earthquake cannot occur in a medium with elevated temperature and low confining pressure (e.g. melted or partially melted rock) because it behaves in a plastic or viscous manner; energy is not accumulated.

Movements along faults are largely controlled by big-scale processes, particularly by the motions of lithospheric plates.

2.2.1. Earthquake parameters

Four basic parameters are used for describing an earthquake. Location (latitude, longitude, depth), origin time and magnitude are the primary earthquake parameters, intensity is additional parameter for describing the earthquake consequences.

2.2.1.1. Location

The location is determined by travel-time curves (dependency of time of wave propagation on epicentral distance). For earthquake location, p wave travel-time is mainly used.

2.2.1.2. Magnitude

Magnitude characterizes the strength of an earthquake. Magnitude reflects a measure of energy of seismic waves released in an earthquake and depends on size of a fault that moves. The determination is based on the maximum amplitude of seismic waves recorded on a seismogram. Once the amplitudes on different seismographs are corrected for the geometric spreading and attenuation it reflects the strength of an earthquake. All magnitude scales have a general form:

$$M = \log_{10} (A/T) + F (h, \Delta) + C,$$

where A is the maximum amplitude of the signal, T is its dominant period, F is the calibrating function for the variation of amplitude with epicentral distance Δ from the seismometer and earthquake depth h, and C is regional scale factor. As can be seen, the magnitude scales are logarithmic (increase in one unit in magnitude reflects ten-fold increase in seismic wave energy). (Stein, 2003)

The local magnitude M_L, referred as "Richter scale", was the first magnitude scale (introduced in 1935 in California). The largest amplitude (often S wave), measured on specific Wood-Anderson seismograph, and the distance between the source and the receiver, given by the difference in the arrival times of the P and S waves, are uniquely related to magnitude. The Richter magnitudes in the original form are no longer used because Wood-Anderson seismographs are rare.

For global studies the body wave magnitude, m_b, and surface wave magnitude M_S were developed. Body wave magnitude is measured usually from the maximum amplitude of the

P wave. The surface wave magnitude, M_S, is determined by measuring of the maximum amplitude of the surface waves.

Although magnitude reflects a measure of energy released in an earthquake it has two major limitations: (1) The magnitude is empirical and it has no direct relation to earthquake physics. (2) Magnitude estimation varies with azimuth (it reflects the amplitude radiation patterns). This can be reduced by averaging results from many stations. The magnitudes do not correctly reflect the size of very large earthquakes (Stein, 2003; Kasahara, 1981).

2.2.1.3. Intensity

Determining macroseismic intensity is one way to characterize ground motions. It is a descriptive measure of the effects of shaking. It depends basically on strength of earthquake, distance from a measuring place to the earthquake hypocenter and geological structure. The most commonly used intensity scales are Modified Mercalli intensity (MMI) scale and European Macroseismic Scale (EMS) ranging from I (nearly unfelt) to XII (destructive earthquake). There is an empirical relation between intensity and magnitude. Intensity determination is based on macroseismic observations; therefore it can be determined even where no seismometers were installed (Stein, 2003).

2.2.2. Focal mechanisms

As mentioned above, a fault is considered to be a planar surface across which relative motion occurs during an earthquake. When the fault is not vertical, the blocks can be classified as: the foot wall block – the lower side of the fault and the hanging wall block – the upper side of the fault. Two basic types of faulting can occur: (1) Strike-slip motion can be either right- or left-lateral. It occurs when the two sides of the fault slide horizontally to each other. (2) Dip-slip faulting occurs as either normal or reverse (thrust) faulting. Normal faulting occurs when the hanging wall block slides downward; in the opposite case, when the hanging wall block slides upward, it causes reverse faulting. At most earthquakes both types of movements occur (pure strike-slip or dip-slip is rare).

The focal mechanism of an earthquake is possible to study with seismograms recorded in various distances and azimuths. The basic principle is that the polarity (direction) of the first P wave arrival varies at different stations. The "up" (compression) polarity means that the station is located such that the material near the fault moves "toward" the station; in

the opposite case the "down" (dilatation) polarity signs that the material near fault moves "away" from the seismometer. These first motions define four quadrants – two compressional and two dilatational. In directions where the first motion changes from compression to dilatation (and the first motion is therefore small or zero) two perpendicular planes (nodal planes) occur. One of the planes is the actual fault plane, the perpendicular auxiliary plane has no relation to real subsurface block distribution. The first motions alone cannot distinguish the actual fault plane and perpendicular auxiliary plane.

These compression-dilatation zones can be plotted on a sphere around the focus. To plot the focal mechanisms in 2D, the lower focal hemisphere transformed to a plane is used. In the final diagram, compressional quadrants are denoted in black and dilatational quadrants in white (Stein, 2003).

2.2.3. Seismic sequences

According to systematic investigation of earthquake sequences, the following three types of behavior are classified. (1) Large earthquake without foreshocks, but frequently followed by aftershocks. This type is common for most large tectonic earthquakes. According to observations, this type occurs in a homogenous medium under nearly uniform applied stress. (2) Large earthquake with foreshocks, followed by numerous aftershocks. Minority of large earthquakes occur this way. Generally it occurs when the structure and/or the spatial distribution of stress are not uniform. (3) The number and the magnitude of the earthquake increases gradually gently with time and decreases after some duration. No predominant shock occurs within the sequence. This type of sequence is called seismic swarm. It occurs in highly inhomogenous medium.

Generally, we presume that the sequence type is dependent on the structural state of earthquake-producing medium (e.g. earth's crust) and the spatial distribution of applied stresses. At shallow depths, the structural state of earth's crust depends on the degree of fracturing. Therefore it is thought that the second type of sequences (foreshocks – principal shock – aftershocks) occurs in moderately fractured regions and the third type (swarms) in highly fractured regions (Mogi, 1967).

2.2.4. Wadati-Benioff zone and its specific features beneath a volcanic arc

The Wadati-Benioff zone is the inclined zone of seismicity delineating the subducting oceanic plate surrounded by mostly aseismic mantle. For the purposes of this study, several important features of the WBZ beneath a volcanic arc are described below. Detailed investigation of variations in slab depth beneath volcanic arcs was made by Syracuse and Abers (2006).

There are some specific features of the seismicity pattern beneath the subduction-related volcanoes which – because of relatively high lateral variability – can be seen only at thin (usually 0,5° and less) cross sections perpendicular to the convergent margin.

In variable depth, commonly between 100 and 200 km, in the Wadati-Benioff zone there is a region without strong earthquakes (M>4). This zone, known as Intermediate Depth Aseismic Gap (IDAG) (Špičák et al., 2004, 2005), is typical for many Wadati-Benioff zones and usually there is a spatial correlation between this zone and volcanism at the surface. The presence of IDAG points to a significant change of material properties within the subducting slab at intermediate depths – the loss of ability of brittle failure which is necessary for strong earthquake presence.

In some cases there is a distinguished seismicity pattern in the overlying mantle wedge growing from IDAG towards a volcano. This is called Seismically Active Column (SAC) (Špičák et al., 2004, 2005). It points to the ability of brittle failure within the overlying wedge. The other important phenomenon is the occurrence of seismic swarms within SAC. The presence of these earthquakes is supposed to be related to the magma transport through the pre-stressed fractured medium.

The presence of IDAG in the Wadati-Benioff zone pointing to a partially melted region in the slab together with presence of SAC pointing to the capability of brittle failure of the fractured medium, favors the position of the source of primary magma below the deepest events of SAC or to the slab (Špičák et al., 2004, 2005).

3. The interaction of subduction-related magma with the overlying mantle wedge

3.1. Introduction

The Sunda-Banda volcanic arc is one of the most seismically as well as volcanically active areas in the world. Therefore, it is a suitable area to study processes at convergent plate margins. The high density of volcanoes within the volcanic arc and plenty of earthquakes form an outstanding dataset sufficient for the research of the relation between earthquake foci distribution and volcanism. A detailed investigation of the earthquake distribution was done in the area of Sunda volcanic arc in order to detect structures related to volcanoes. This study is based on several main conclusions. (1) The spatial distribution of earthquake foci in the Wadati-Benioff zone is not homogenous. In depths between 100 and 200 km the presence of the Intermediate Depth Aseismic Gap was commonly proved. The width and the depth of this gap are variable but there are no subduction-related volcanoes which cannot be correlated with this aseismic zone. The localization of the IDAG is related to the position of volcanic chain at the surface. (2) Earthquakes outside the Wadati-Benioff zone can be usually assigned to one of seismically active fracture zones of regional character. Fault plane solutions of the earthquakes determine basic parameters of the fracture zones and differ from those occurring in the Wadati-Benioff zone. (3) Earthquake clusters (SAC) were found beneath 9 from 14 active volcanic domains in the region. The cause of occurrence of earthquakes in a cluster is considered to be connected with the magma intrusion into the fracture zone, which is subcritically prestressed by the process of subduction. (4) The presence of IDAG in the subducting slab and SAC within the overlying wedge favors to the position of the source of primary magma below the deepest events of SAC or in the slab (Špičák et al., 2005).

In this study I would like to continue in investigation of shallow events in the Banda arc and describe the seismicity related to volcanoes in the whole complex of the Sunda-Banda volcanic arc. Contrary to the previous research the attention has been paid more to the character of earthquake clusters beneath the volcanoes than to the features of the Wadati-Benioff zone.

3.2. Area of interest

The area was selected with respect to the previous research which was conducted in the central part of the Sunda Arc (Java, Nusa Tenggara) (Fig. 2). In the area 3° S – 12° S and 105° E – 125° E, 14 active volcanic domains were investigated (from west to east: Gedeh, Guntur, Slamet, Merapi, Kelut, Raung, Batur, Rinjani, Tambora, Sangeang, Ranakah, Paluweh, Lewotobi, Sirug) (Špičák et al., 2005).

Ten volcanoes within the area 4° N – 10° S and 124° E – 134° E were considered for the purposes of the present study: Emperor of China, Nieuwerkerk, Gunungapi Wetar, Wurlali, Teon, Nila, Serua, Manuk, Banda Api and Colo (Fig. 2). Excluding Colo volcano, the volcanoes belong to the Sunda-Banda volcanic arc. The Colo volcano was included to this study because of a specific tectonic position and spatial relation to other volcanoes (Neumann Van Padang, 1951; Siebert, 2002-; Venzke, 2002-).

The selected area is of a very complicated geodynamical character (Fig. 3). The subduction of Indo-Australian Plate under the Eurasian Plate (related volcanoes: Emperor of China, Nieuwerkerk, Gunungapi Wetar, Wurlali, Teon, Nila, Serua, Manuk) has been probably influenced by the collision of Indo-Australian continental lithosphere. From the northeast the oceanic lithosphere of Pacific Plate subducts under the Eurasian Plate (Banda Api). From the north to the south the oceanic lithosphere of the Philippine Plate subducts under the Eurasian Plate (Colo).

3.3. Data

3.3.1. EHB database

The Engdahl database, denoted as EHB, contains determinations of the International Seismological Center (ISC) during 1964 – 2007 period relocated by the algorithm of Engdahl et al. (1998). The production of EHB database is described below.

3.3.1.1. International station network

The list of contributing stations contains nearly 10 000 stations and is maintained jointly by International Seismological Center and the World Data Center for Seismology, Denver (WDC), which is operated by the US National Earthquake Information Center (NEIC).

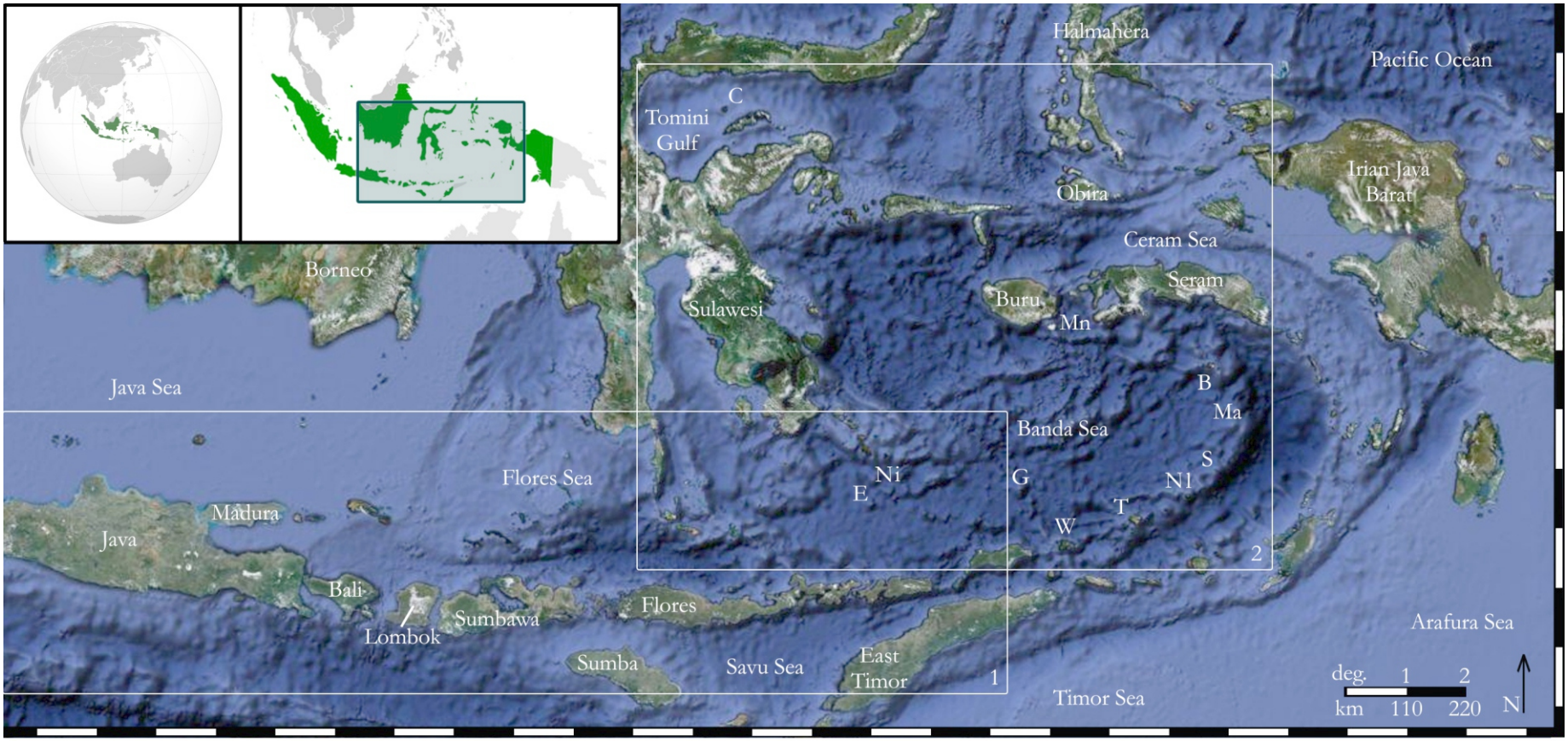

Fig. 2. The geographical map of the eastern Indonesia region. The area of research is denoted by white rectangles (1 – previous research (Špičák et al., 2005), 2 – this research), positions of volcanoes Emperor of China (E), Nieuwerkerk (Ni), Gunungapi Wetar (G), Wurlali (W), Teon (T), Nila (Nl), Serua (S), Manuk (Ma), Banda Api (B), Colo (C) and Manipa Basin (Mn) are denoted by letters.

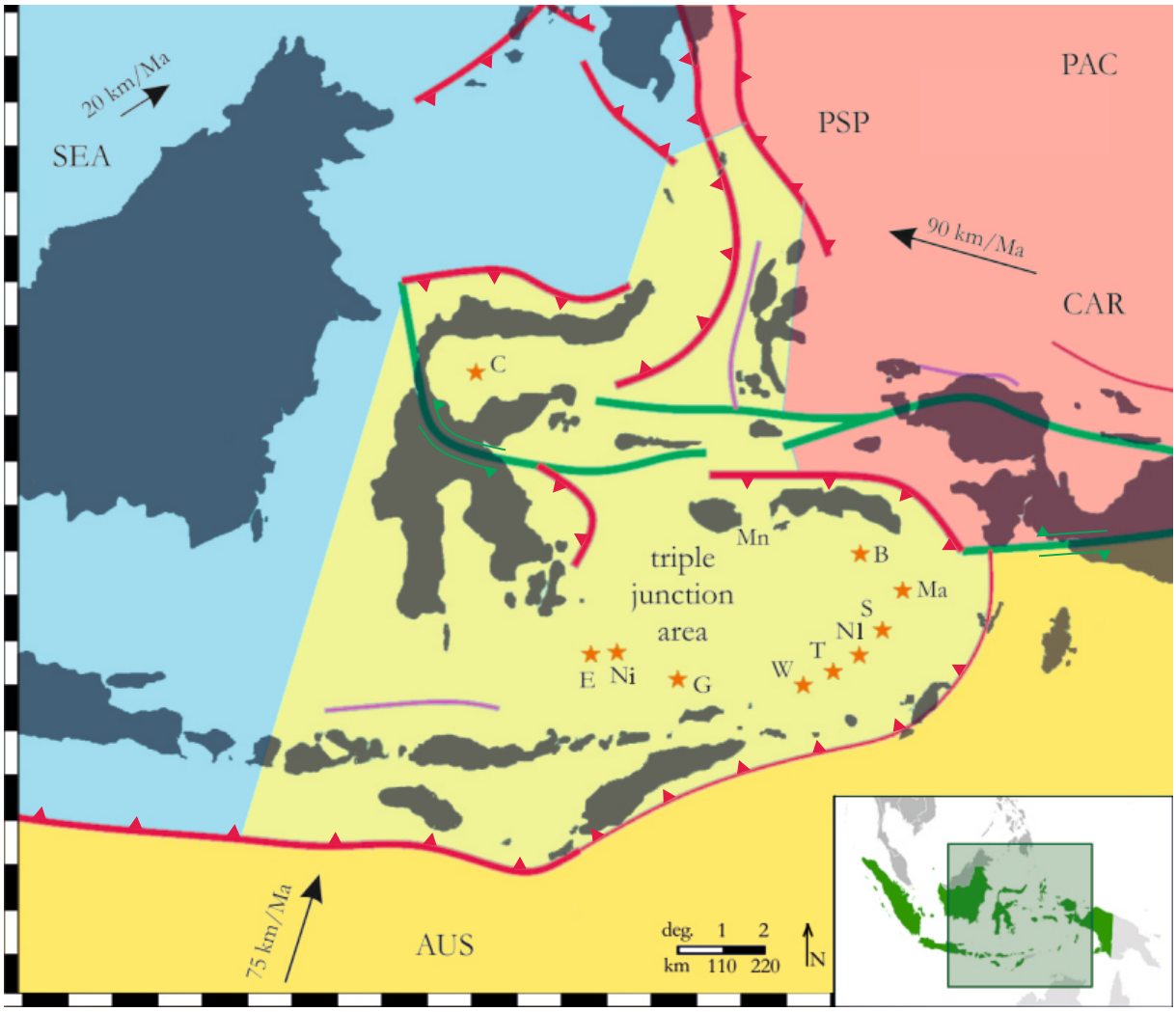

Fig. 3. The tectonic map of the eastern Indonesia region. Active subduction zones are denoted by thick red lines, inactive by thin red lines, major strike slip faults by green lines, thrust faults by violet lines. Tectonic plate of South-East Asia (SEA) is blue colored, Pacific plate (PAC), Caroline plate (CAR) and Philippine Sea plate (PSP) are red, Australian plate (AUS) is yellow and green is the triple junction area. Velocity and direction of the plate motion is denoted by black arrow. Positions of volcanoes Emperor of China (E), Nieuwerkerk (Ni), Gunungapi Wetar (G), Wurlali (W), Teon (T), Nila (Nl), Serua (S), Manuk (Ma), Banda Api (B), Colo (C) are denoted by orange stars, position of Manipa Basin (Mn) by letters.

The primary purpose of the station list is to include the station to the international context by giving a unique code to each station. The codes are 3 to 5 character alphanumerical sequences and cannot be re-used when the station is abolished. When the station is no longer in operation it still remains in the list but it is marked as "closed".

The number of stations actually in use is around 2800. The geographic distribution of reporting stations is non-uniform. Generally, the highest station density is in the seismically active and economically well-developed regions such as west coast of USA, South Europe and Japan (about 500 stations per 10^6 km^2). On the other hand we can see insufficient density in seismically active regions such as Hindu Kush – Pamir or Southeast Asia region (according to the data from 2001 the density varies between 1 and 5 stations per 10^6 km^2). Lack of the reporting stations is also in Fiji, or Mexico-Guatemala (Willemann, 2001).

3.3.1.2. International Seismological Center

Contributing organizations controlling regional station networks read recordings of stations, associate the readings of local and regional events and compute preliminary locations. Contributing organizations are systematized in similar registry as stations. Over 250 organizations are registered, but like in station registry, many of codes are disused. Only about 60 organizations are actually contributing. The preliminary results are sent to the ISC to final analysis. When all the data are collected, the ISC database is produced (Willemann, 2001).

3.3.1.3. EHB procedure

Although the ISC database is useful for seismic hazard assessment, the data cannot be confidently applied for resolving structural problems. The main reason is the variable level of focal depth mislocations that are caused particularly by errors in the reference Earth model and phase misidentifications. This bias can be significantly reduced by using a proper reference Earth model, by improving the usage of data and constraining the data only to those that are teleseismically well distributed. These corrections are constituents of the Engdahl et al. (1998; EHB) algorithm, which is used for improving routine hypocenter determinations from the ISC database. The bias in hypocenter determination is reduced in the final database; on the other hand, a lot of events with small magnitude are lost.

It is not possible to set the lower limit of the magnitude range theoretically, but, empirically the earthquakes are tabulated for $m_b>4$. In some cases the magnitude is not computed. The focal position and depth accuracy is the fundamental factor for our further work with the

data. The range of the error in the whole EHB database is commonly between 5 and 25 km for the position and between 2 and 15 km for the depth.

This relatively high accuracy and robustness of the determinations in conjunction with a huge number of data within the database enables us to use these data for structural analysis of the Earth interior.

3.3.2. Global centroid moment tensor solution

Global Centroid Moment Tensor Solutions (GCMTS) database of earthquake focal mechanisms maintained by Lamont-Doherty Earth Observatory (LDEO) of Columbia University was used in range since 1976 - 2007.

3.3.3. Other data used

The Catalogue of the Active volcanoes of the World (Neumann Van Padang, 1951), Database of volcanoes and Smithsonian Global Volcanism program database (Siebert et al., 2002-, Ventzke et al., 2002-) were the sources of information on the volcanoes. Information about petrological character of lavas was taken from the Catalogue of the Active volcanoes of the World or from individual papers.

3.4. Method

The seismicity pattern of the subducting plate and the seismic activity of the region as a whole were studied by covering the region by narrow vertical swaths perpendicular to the trench. Azimuth and length of the swaths were variable; width of each cross section was set at 0.5 degree (circa 55 km). Three parallel cross sections form a rectangular area around a volcano, which is placed in the middle of the central section. Plotting the data from these cross sections to length-depth plots helps us to distinguish the events occurring in the Wadati-Benioff zone and those in the overlying plate.

From the events within the vertical sections the shallow events occurring in the overlying lithospheric wedge were selected. The maximum depth of selected earthquakes was commonly less than 100 km; in the lengthwise direction the selection was limited by the expected border between the subducting slab and the overlying mantle wedge in order to cut

off all events occurring in the Wadati-Benioff zone. The epicentral map with GCMTS fault plane solutions was created in order to find out the orientation of stresses causing the earthquakes. The correlation between the underlying seismic activity and observed volcanic eruptions was also tested.

3.4.1. Searching for earthquake sequences

Earthquake sequences were searched within the dataset of shallow events occurring in the overlying wedge by using MS Excel 2010 procedure. For our purposes as the earthquake sequence was considered the group (n>4) of earthquakes occurring in the area smaller than 1° x 1° with the pause between two neighboring events less than 10 days. The algorithm basically consists of two steps: (1) computing time differences between neighboring earthquakes in the time-ordered database, and if it is less than 10 days (2) computing the closeness (reverse value of distance) of these events. High values of the closeness indicate the presence of the earthquake sequence.

3.5. Volcanic domains

For the purposes of the analysis the studied area was divided into four domains according to the geographic distribution of volcanoes (Fig. 4). The domains will be discussed from south-west of the area of interest counter clockwise to north-west. Numbers of volcanoes were taken from the database of Global Volcanism Program (Siebert et al., 2002-).

3.5.1. Domain 1

The westernmost domain consists of two submarine volcanoes denoted as "uncertain" by Ventzke et al. (Ventzke et al., 2002-); Emperor of China, Nieuwerkerk and one subaerial volcano; Gunungapi Wetar.

- **Emperor of China** (no. 0605-01=; lat. 6.617 S; lon. 124.217 E, alt. -2850 m)

Emperor of China is a submarine volcano situated in the south-west corner of the Banda Sea (Siebert, 2002-; Venzke, 2002-). Like Gunungapi Wetar and Nieuwerkerk, Emperor of China does not belong to the active Sunda-Banda volcanic arc. Belonging to the list of active volcanoes is questionable.

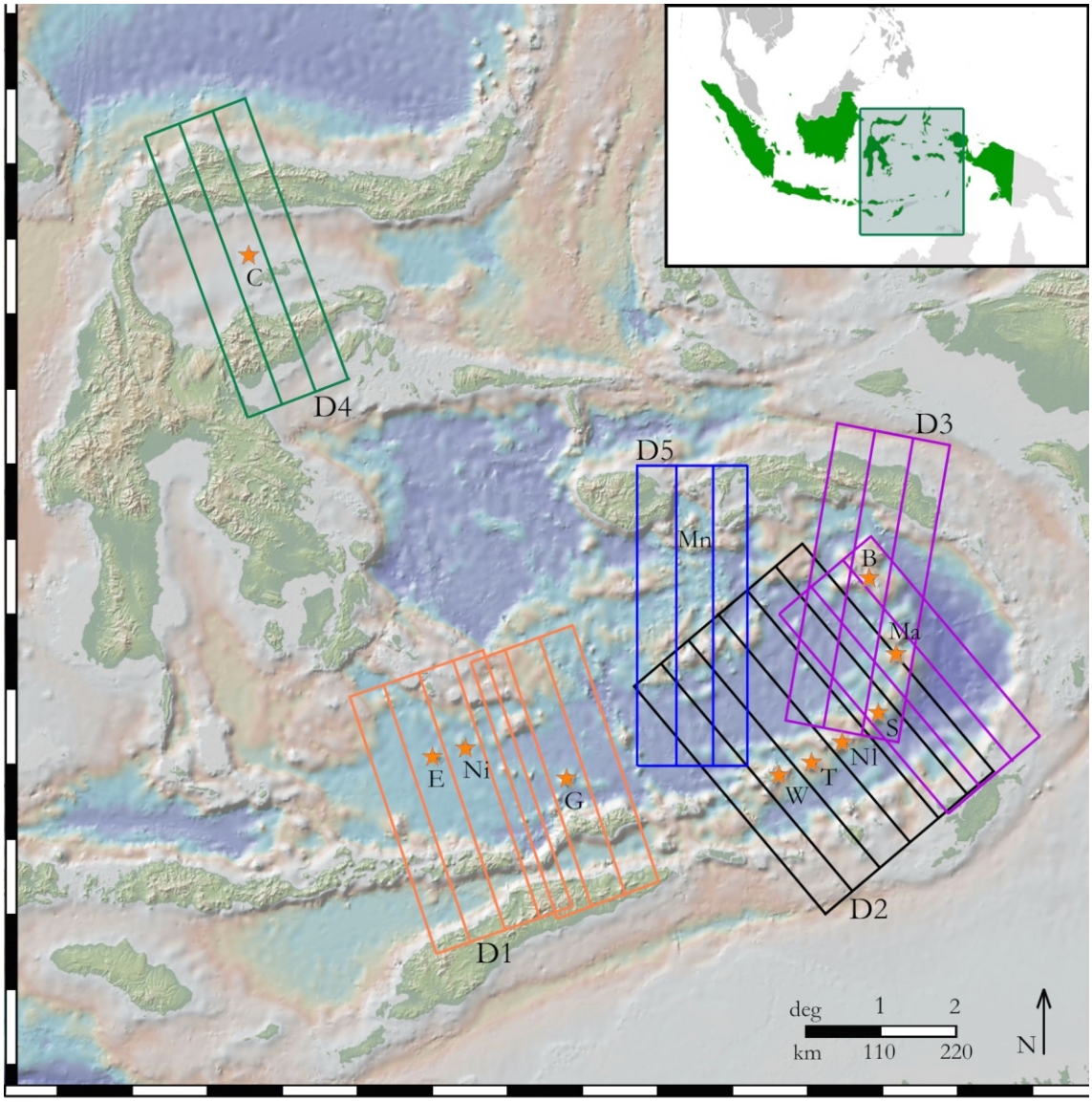

Fig. 4. The geographical map of the eastern Indonesia region. Volcanic domains D1, D2, D3, D4, D5 are denoted by colored rectangles, positions of volcanoes Emperor of China (E), Nieuwerkerk (Ni), Gunungapi Wetar (G), Wurlali (W), Teon (T), Nila (Nl), Serua (S), Manuk (Ma), Banda Api (B), Colo (C) by orange stars; position of Manipa Basin (Mn) is denoted by letters.

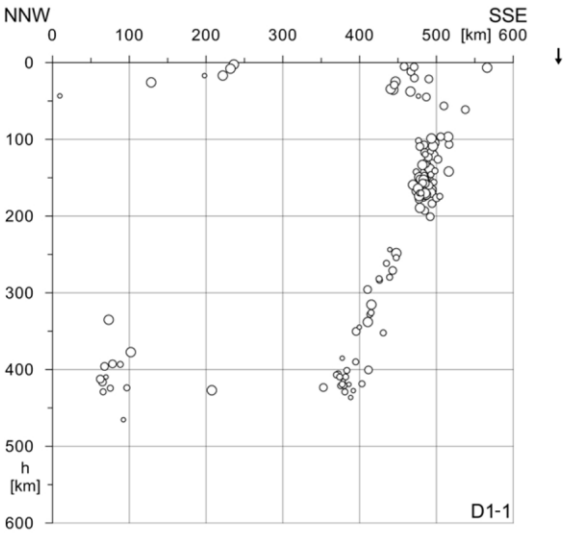

Fig. 5. Vertical sections D1-1, D1-2, D1-3, D1-4, D1-5, D1-6, D1-7 perpendicular to the trench. h – focal depth, black and white triangles - position of volcanoes (G: Gunungapi Wetar, N: Nieuwerkerk, E: Emperor of China), black arrow - position of the trench. Symbol size reflects body wave magnitude in the EHB database.

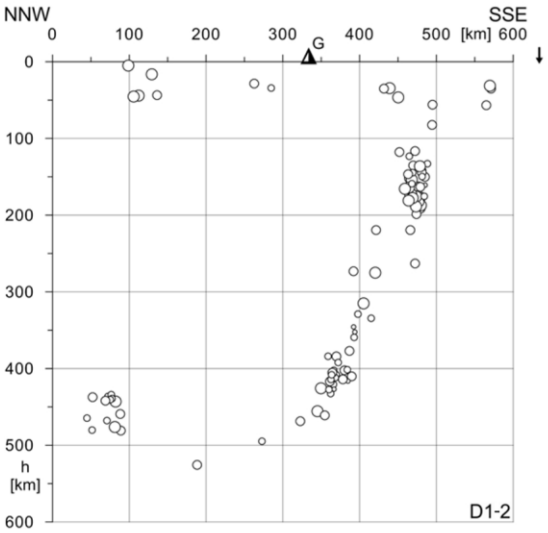

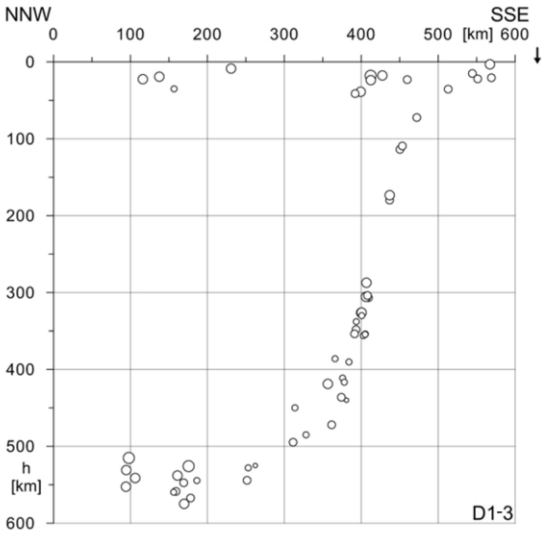

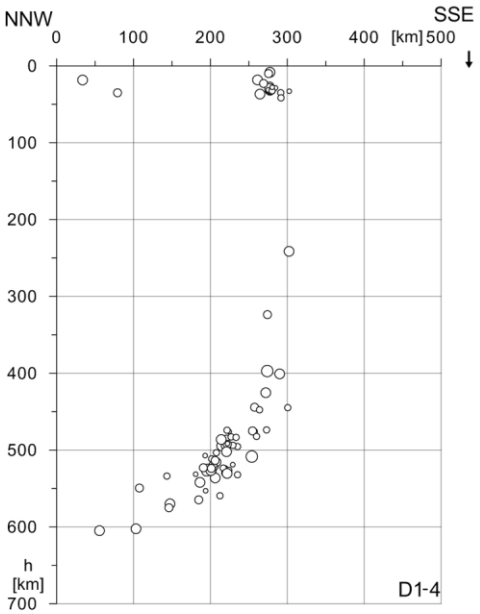

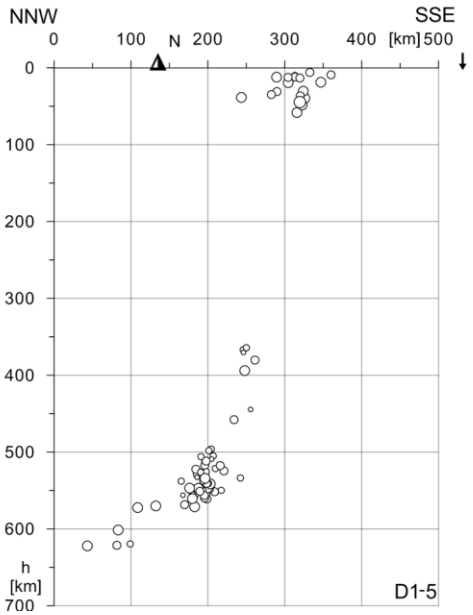

cont.

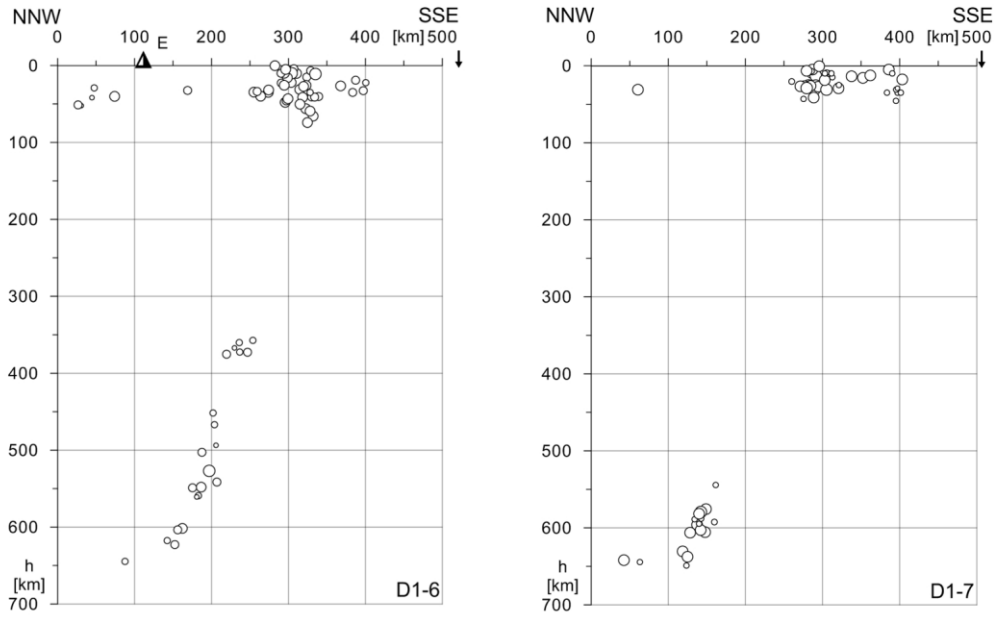

- **Nieuwerkerk** (no. 0605-02=; lat. 6.6 S; lon. 124.675 E, alt. -2285)

Submarine volcano Nieuwerkerk is situated about 50 km west of Emperror of China and is of a similar character. (Siebert, 2002-; Venzke, 2002-)

- **Gunungapi Wetar** (no. 0605-03=; lat. 6.642 S; lon. 126.65 E, alt. 282 m)

The Gunungapi Wetar stratovolcano forms a small, roughly circular island with a cone in the central crater. Because of the high inclination of the slopes, three great landslides are visible. Like other volcanoes in the first domain, Gunugapi Wetar does not belong directly to the active Sunda-Banda volcanic arc. Two eruptions have been recorded in historical times (1512, 1699) (Siebert, 2002-; Venzke, 2002-). The volcano is formed by andesitic lavas. (Neumann Van Padang, 1951)

3.5.1.1. Seismicity in the domain

Four cross-sections were delimited around Nieuwerkerk and Emperor of China volcanoes and three around Gunungapi Wetar volcano in the azimuth of 330°. No earthquakes have been observed beneath these volcanoes. (Fig. 5)

3.5.2. Domain 2

Four volcanoes (Wurlali, Teon, Nila, Serua) of the Sunda-Banda volcanic arc belong to this Domain, chained in the NE-SW trending line (Fig. 6 (a)).

- **Serua** (no. 0605-07=; lat. 6.3 S; lon. 130 E, alt. 641 m)

The stratovolcano Serua is one of the most active volcanoes of the Sunda-Banda volcanic arc, with 12 eruptions recorded since 1683. The last volcanic episode was recorded in September 1921 (Siebert, 2002-; Venzke, 2002-). The lava is of andesitic character. (Neumann Van Padang, 1951)

- **Nila** (no. 0605-06=; lat. 6.733 S; lon. 129.5 E, alt. 781 m)

Nila Island formed by a 8 x 10 km caldera with a low rim approximately at a sea level. A 5x6 km cone is placed roughly in the middle of the caldera. Nila is an andesitic volcano where several phreatic eruptions from summit vents were observed. Four eruptions were recorded during the 20th century (Siebert, 2002-; Venzke, 2002-).

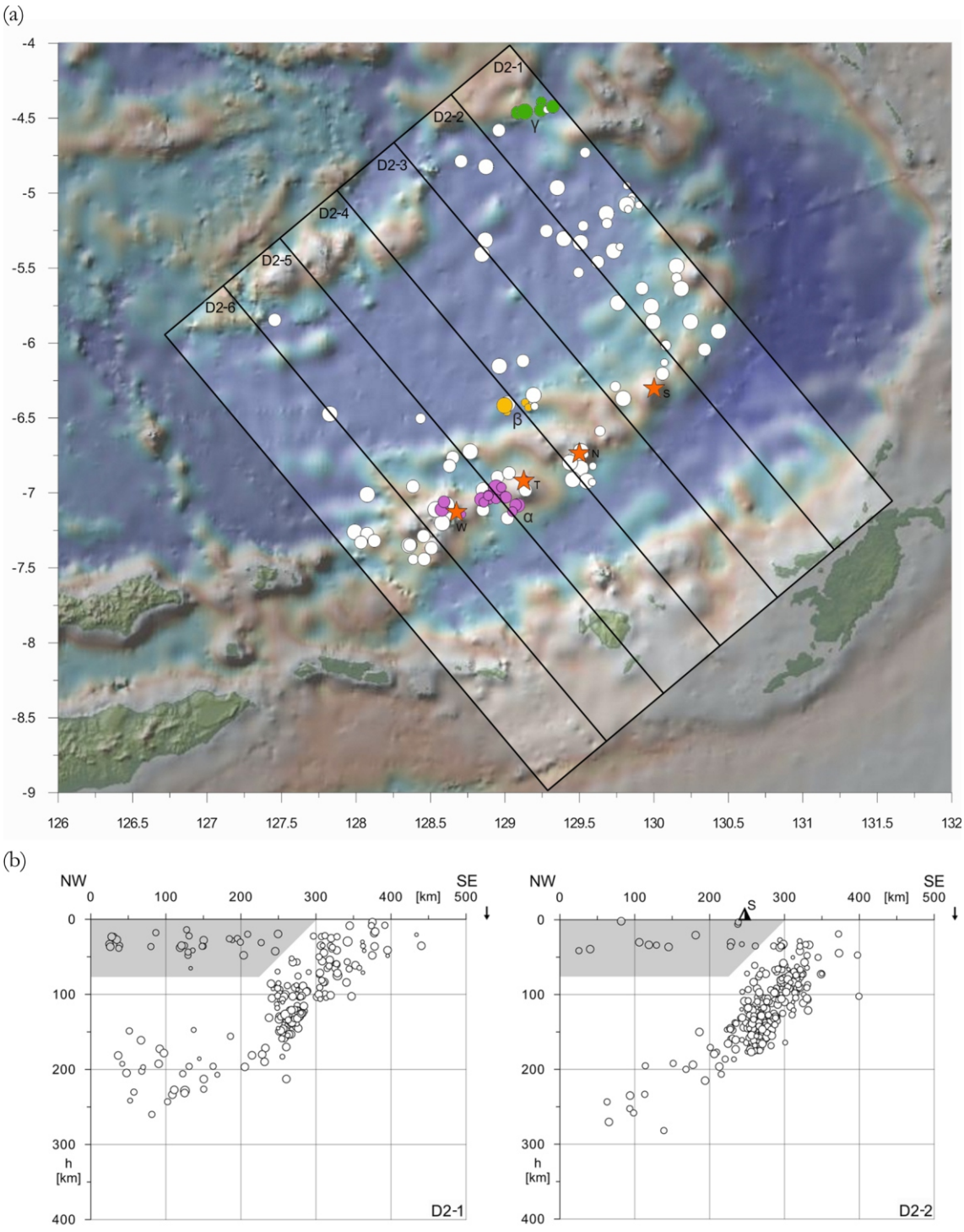

Fig. 6. (a) Epicentral map of selected shallow earthquakes in Domain 2. Vertical sections D2-1, D2-2, D2-3, D2-4, D2-5, D2-6 are denoted by rectangles, volcanoes Wurlali (W), Teon (T), Nila (N) and Serua (S) by red star. Earthquake sequences are marked by letters α, β, γ. (b) Vertical sections D2-1 – D2-7 perpendicular to the trench. h – focal depth, black and white triangles - position of volcanoes, black arrow - position of the trench. Symbol size reflects body wave magnitude in the EHB database. (c) Fault plane solutions of GCMTS. Bounded diagrams belong to events from earthquake clusters.

(b) cont.

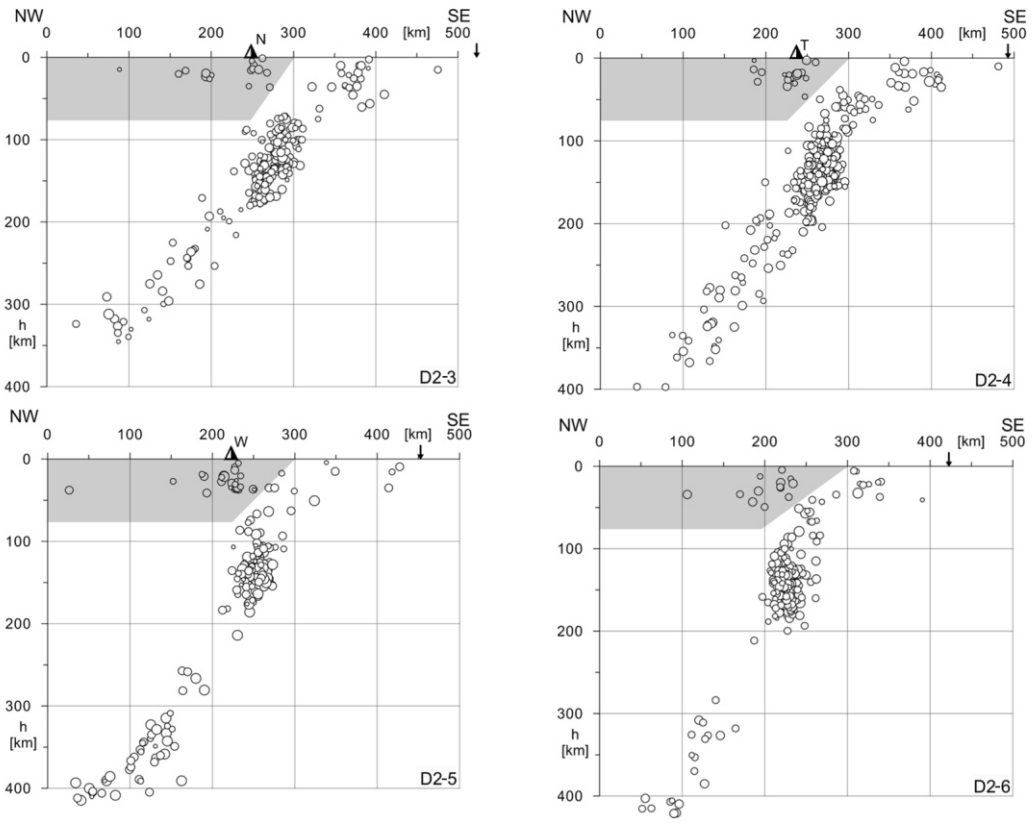
NW
SE
0
100
200
300
400
[km]
500
N
T
W
h
[km]
D2-3
D2-4
D2-5
D2-6

(c)

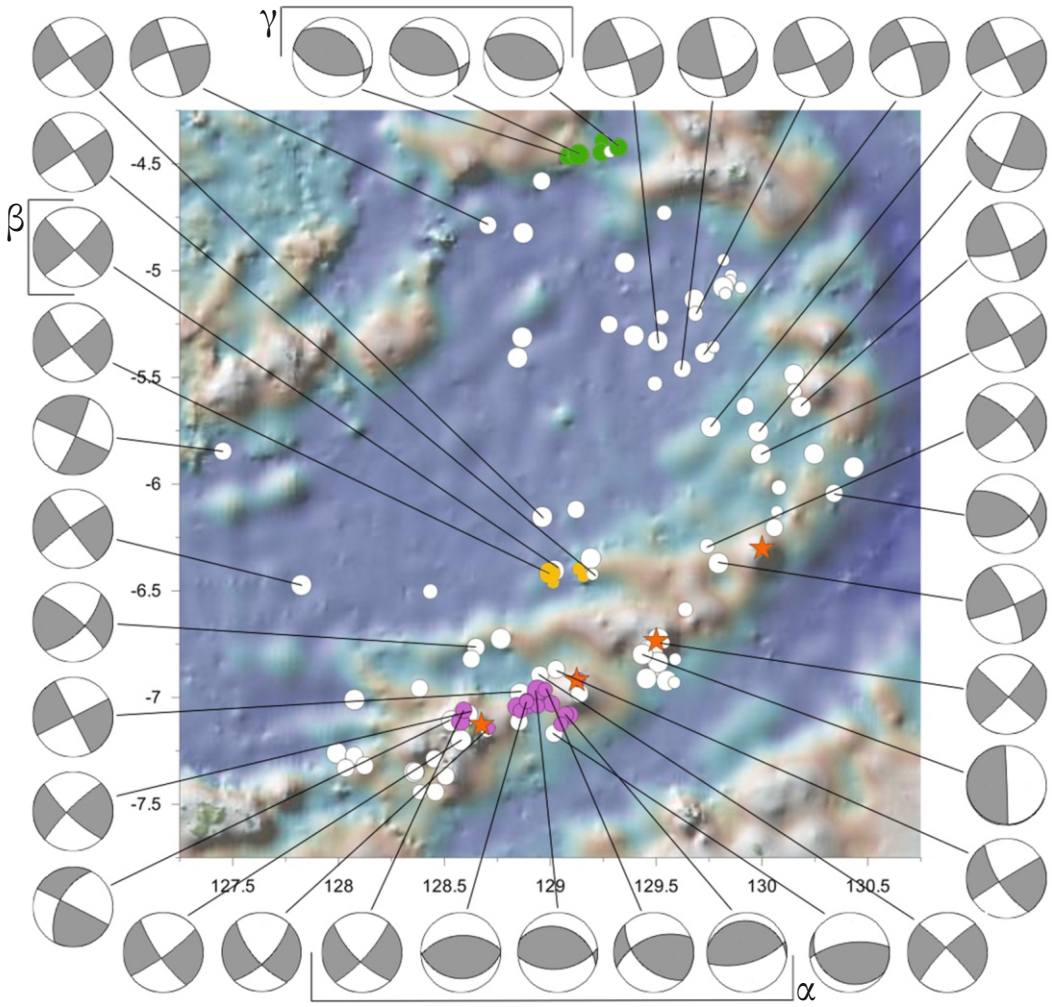
γ
β
α
-4.5
-5
-5.5
-6
-6.5
-7
-7.5
127.5
128
128.5
129
129.5
130
130.5

- **Teon** (no. 0605-05=; lat. 6.916 S; lon. 129.125 E, alt. 655 m)

Five eruptions have been recorded since 1659 at this in the NNE direction elongated volcano (Siebert, 2002-; Venzke, 2002-). The lavas are of andesitic character (Neumann Van Padang, 1951).

- **Wurlali** (no. 0605-04=; lat. 7.125 S; lon. 128.675 E, alt. 868 m)

Wurlali stratovolcano is situated on the Damar Island. The volcano is placed in the 5 km caldera structure and is made of andesitic lava. The only known historical eruption dates back to 1892. Fumarolic activity occurs in twin summit craters, producing exploitable sulfur deposits. (Siebert, 2002-; Venzke, 2002-)

3.5.2.1. Seismicity in the domain

Six cross sections in the azimuth of 320° covered the Domain 2 area. One hundred nine earthquakes occurred within the overlying lithospheric wedge in this domain in the magnitude range 3.2 – 6.2. The focal depth varies from the surface to 75 km. Three earthquake sequences were found within this dataset (Fig. 6 (a), (b)).

The GCMTS fault plane solutions were calculated for 28 events which are not within the sequences. The strike-slip faulting dominates. The strike-slip character is probably related to the expected NW-SE trending fracture zone (Fig. 6 (c)).

- The 1998 sequence (Fig. 6 (a), λ)

The largest sequence of earthquakes in this volcanic domain contains 17 events that occurred in 13 days. The sequence started on November 9th, 1998 when 10 events occurred, continued by 2 events on November 10th and 3 events on November 11th; the last event was recorded on November 21st. The earthquake hypocenters were located at depth between 5 and 50 km. The magnitude of the strongest event reached m_b 6.2 (second event on November 9th), other calculated magnitudes reached a value from 3.9 to 5.9. According to definitions we consider it to be the principal shock followed by an aftershock sequence. The center of the sequence was situated between Wurlali and Teon volcanoes. No time-depth dependence was found in this swarm. No volcanic activity was reported that could be related to this seismic activity. The GCMTS fault plane solutions were calculated for five events. In contrast to other mechanisms of this domain the thrust fault mechanism predominates.

- The 1974 sequence (Fig. 6 (a), β)

The sequence consists of four events that occurred in 2 days between March 6th and 7th, 1974. Events were shallow, with focal depth between 2 and 27 km. Magnitude was calculated only for one event and reached a value of 5.7. The epicenters of the events were situated about 60 km north of Teon volcano and 50 km north-west of Nila volcano. Origin time of the 1974 earthquakes does not correspond with any volcanic activity of volcanoes of Domain 2. The GCMTS fault plane solutions were calculated for one event; it is of strike-slip character.

- The 2007 sequence (Fig. 6 (a), γ)

This sequence contains five events that occurred in 6 days between August 17th and 22nd, 2007. The focal depth varies between 22 and 37 km. The magnitude reaches from 4.2 to 6. This sequence is situated approximately 75 km south from the Banda Api volcano. No volcanic activity that could be related to this seismic activity was reported. The GCMTS fault plane solutions were calculated for three events. Two of them are dominantly of strike slip character; the third one is of thrust fault character.

3.5.3. Domain 3

The Domain consists of one recently active volcano named Banda Api and one late quaternary volcano called Manuk. They both belong to the Sunda-Banda volcanic arc (Fig. 7 (a)).

- **Banda Api** (no. 0605-09=; lat. 4.525 S; lon. 129.871 E, alt. 640 m)

The volcano, denoted as the northernmost volcano in the Sunda-Banda volcanic arc is situated on one of three islands called Naira in the north-eastern part of the Banda Sea. The islands represent the subaerial components of mostly submerged, 7 km in diameter caldera. It is supposed that there were at least two episodes of caldera formation; arcuate islands called Lonthor and Naira are considered to be the fragments of the pre-caldera volcanoes. Over 25 eruptions of Banda Api have been recorded since 1586, mostly of explosive character. The last activity of the andesitic volcano was recorded in 1988 (Siebert, 2002-; Venzke, 2002-).

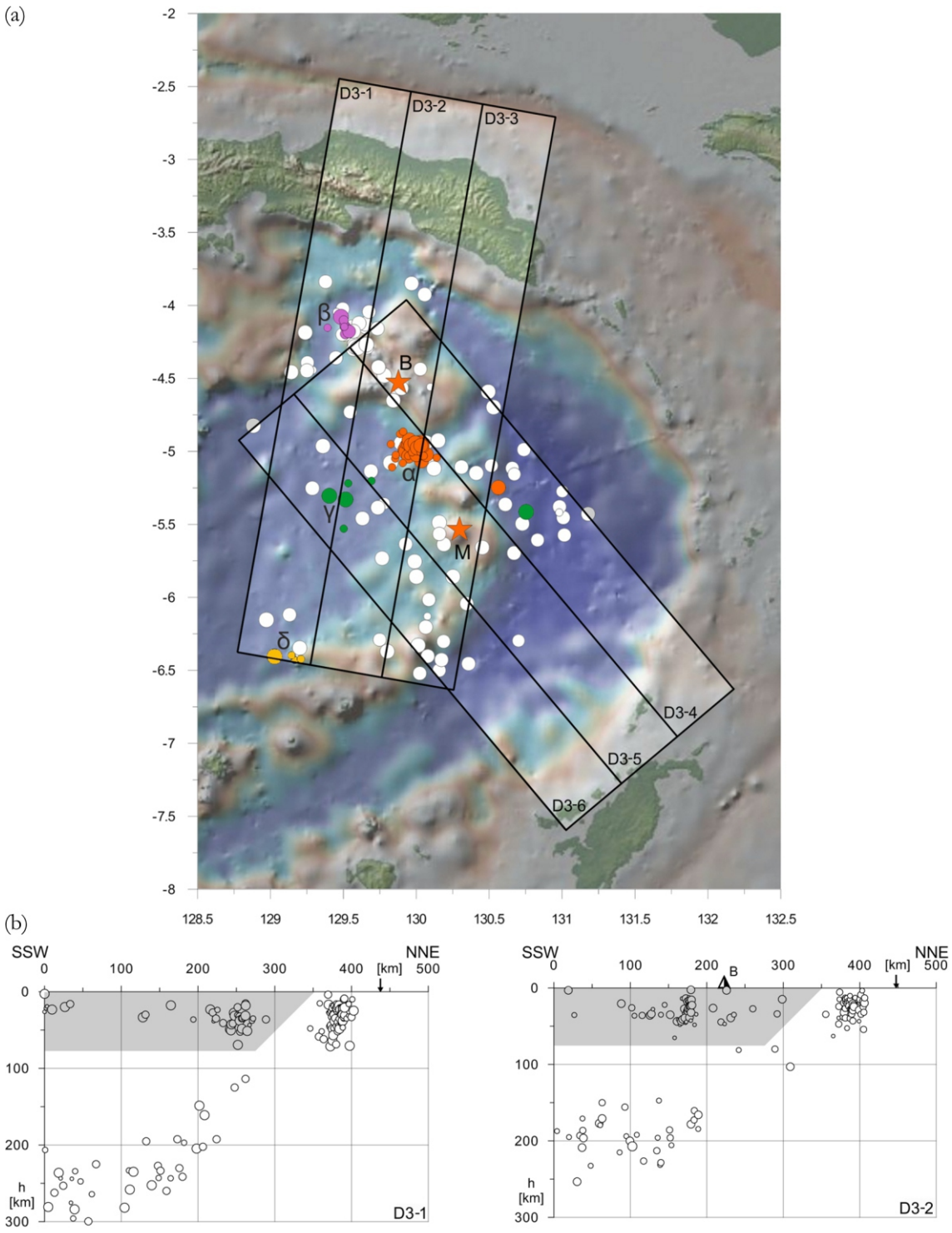

Fig. 7. (a) Epicentral map of selected shallow earthquakes in Domain 3. Vertical sections D3-1, D3-2, D3-3, D3-4, D3-5, D3-6 are denoted by rectangles, volcanoes Manuk (M), Banda Api (B) by red star. Earthquake sequences are marked by letters α, β, γ, δ. (b) Vertical sections D3-1 – D3-6 perpendicular to the trench. h – focal depth, black and white triangles - position of volcanoes, black arrow - position of the trench. Symbol size reflects body wave magnitude in the EHB database. (c) Fault plane solutions of GCMTS. Bounded diagrams belong to events from earthquake clusters.

(b)cont.

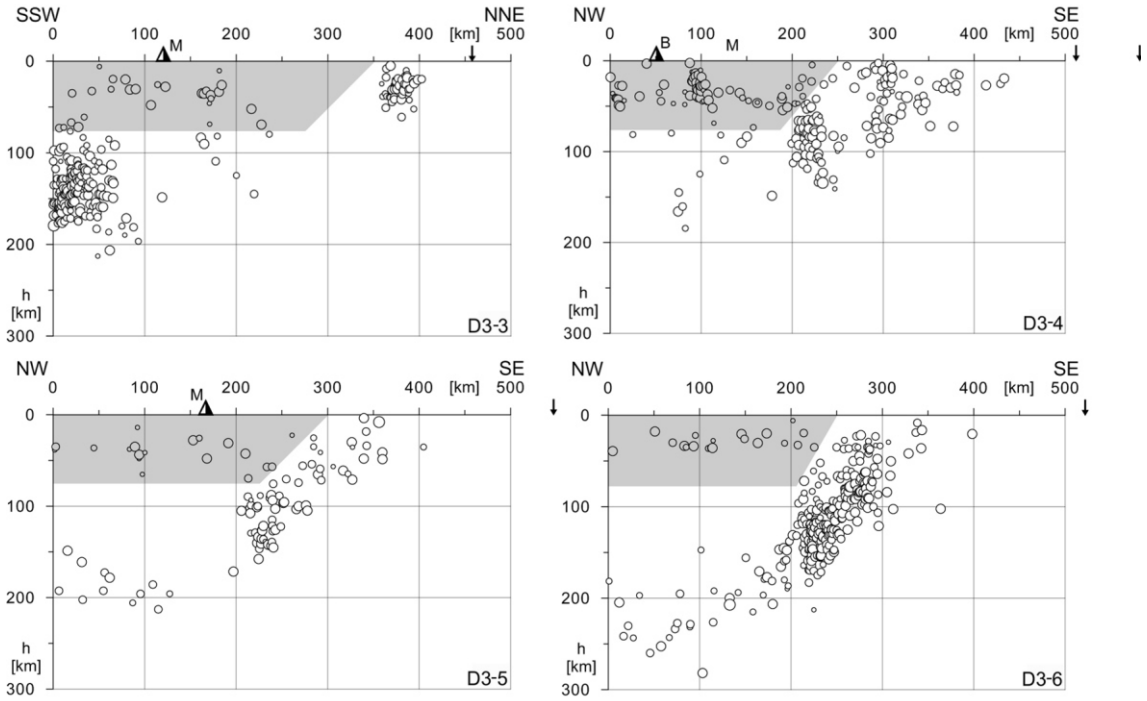
SSW
NNE
NW
SE
0
100
200
300
400
[km]
500
M
B
h
[km]
300
D3-3
D3-4
D3-5
D3-6

(c)

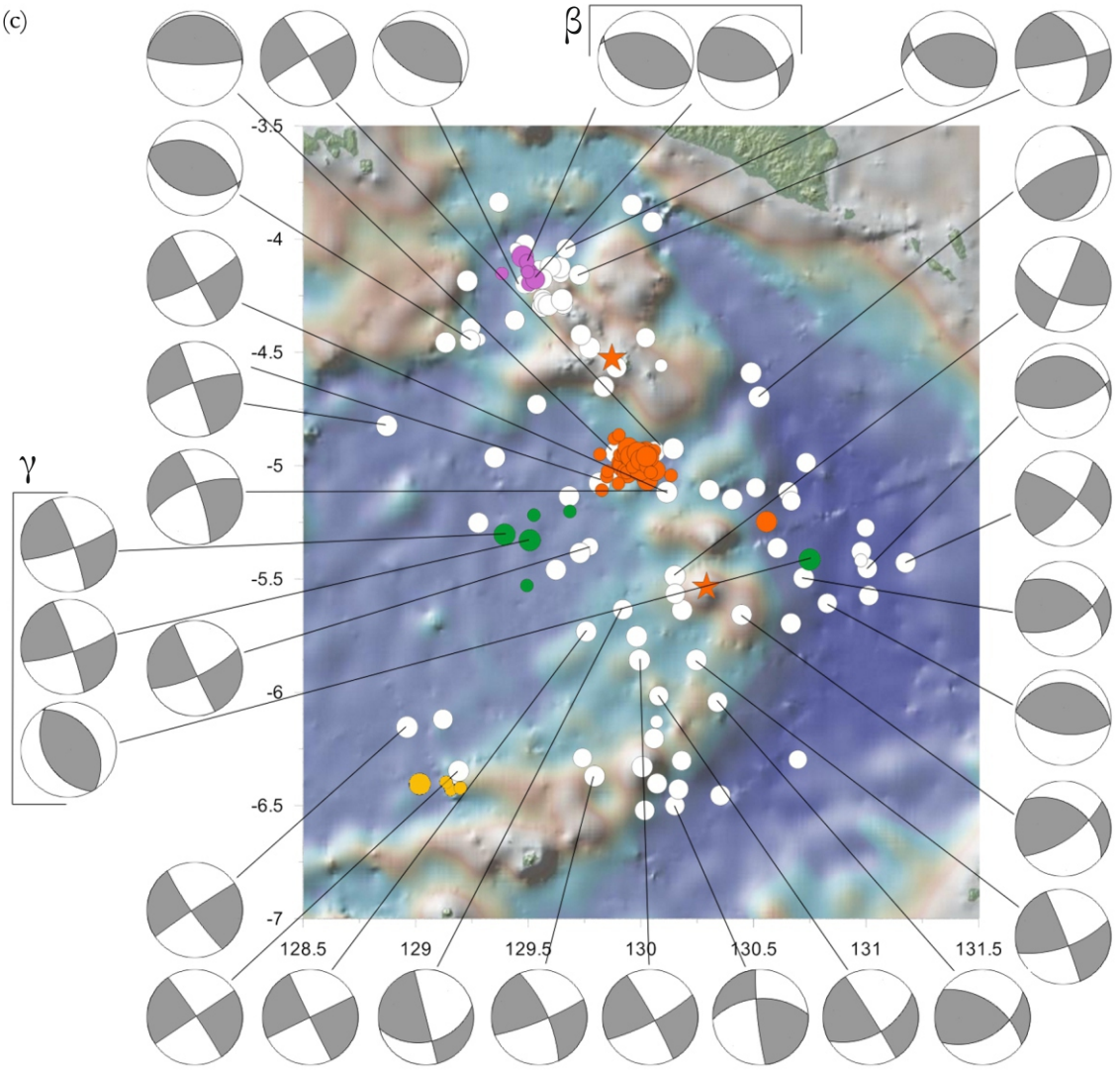
β
γ
-3.5
-4
-4.5
-5
-5.5
-6
-6.5
-7
128.5
129
129.5
130
130.5
131
131.5

- **Manuk** (no. 0605-08=; lat. 5.533 S; lon. 130.292 E, alt. 282 m)

Manuk is the easternmost volcano in the arcuate Sunda-Banda volcanic arc. No eruption of this andesitic volcano has been recorded in historical times (Siebert, 2002-; Venzke, 2002-; Neumann Van Padang, 1951).

3.5.3.1. Seismicity in the domain

The domain contains 442 events that belong to the wedge overlying the subducting slab. Two systems of cross sections were constructed, situated in the azimuth of 320° (around Manuk volcano) and in the azimuth of 10° (around Banda Api volcano). The focal depth varies from the surface to 75 km. The magnitude range is 3.2 – 6.2. Four earthquake sequences were found within this dataset (Fig. 7 (a), (b)).

The GCMTS fault plane solutions were calculated for 27 events which are not within the sequences. NE-SW trending strike-slip mechanisms dominate, one third of plane solutions was of significant dip-slip character. No significant difference between mechanisms of events from the sequences and of other events was found (Fig. 7 (c)).

- The 1974/1975 sequence (Fig. 7 (a), λ)

At least thirty-seven earthquakes occurred during the most significant sequence of the Domain 3 dataset during nearly 4 months at the turn of the years 1974 and 1975. The sequence started on December 2nd, 1974 and ended on March 19th, 1975. The activity was almost uniform in time during the whole period with 2 events per week, only at the beginning of February the activity was approximately twice as high. The focal depth varies between 10 and 70 km. No earthquake was smaller than m_b 5.1; the strongest one was m_b 6; the most common magnitude was between 5.2 and 5.6. These numbers are influenced by the fact that for 18 from 37 events magnitude was not calculated. The sequence is situated between Banda Api and Manuk volcanoes. No volcanic activity that could be related to this seismic activity was reported. The sequence occurred earlier than GCMTS fault plane solutions started to be calculated.

- The 1993 sequence (Fig. 7 (a), β)

The sequence consists of eight events that occurred in 3 days between January 3rd and 5th, 1993. The focal depth varies between 15 and 70 km. The magnitude reaches from 4.8 to 5.8. The epicenters of the events were situated north-west of Banda Api volcano. No volcanic activity that could be related to this seismic activity was reported. The GCMTS fault

plane solutions were calculated for two events. In contrast to other mechanisms of this domain the thrust fault mechanism predominates.

- The 1974 sequence (Fig. 7 (a), γ)

The sequence consists of four events that occurred in 2 days between March 6th and 7th, 1974. Events were shallow, with focal depth between 2 and 27 km. Magnitude was calculated only for one event and reached a value of 5.7. The epicenters of the events were situated about 60 km north of Teon volcano and 50 km north-west of Nila volcano. Origin time of the 1974 earthquakes does not correspond with any activity of volcanoes of Domain 2. The GCMTS fault plane solution was calculated for one event; it is of strike-slip character.

- The 2007 sequence (Fig. 7 (a), δ)

This sequence contains five events that occurred in 6 days between August 17th and 22nd, 2007. The focal depth varies between 22 and 37 km. The magnitude reaches from 4.2 to 6. This sequence is situated approximately 75 km south from the Banda Api volcano. No volcanic activity that could be related to this seismic activity was reported. The GCMTS fault plane solutions were calculated for three events. Two of them are dominantly of strike slip character; the third one is of thrust fault character.

3.5.4. Domain 4

This Domain consists of one active volcano named Colo. (Fig. 8 (a)). The volcano is related to the North Sulawesi Trench where South-East Asia plate subducts under lithosphere of the triple junction area.

- **Colo** (no. 0606-01=; lat. 0.167 S; lon. 121.608 E, alt. 507 m)

Colo stratovolcano is situated in Sulawesi in the central area of the Gulf of Tomini and forms a small island called Una Una. Only three eruptions have been recorded in historical times (1898, 1938, 1983). All of them were of explosive character (Siebert, 2002-; Venzke, 2002-). The island is built of andesitic lavas (Neumann Van Padang, 1951).

3.5.4.1. Seismicity in the domain

Three cross sections in the azimuth of 340° covered the Domain 4 area. Ninety-three earthquakes occurred within the overlying lithospheric wedge in this domain in the magni-

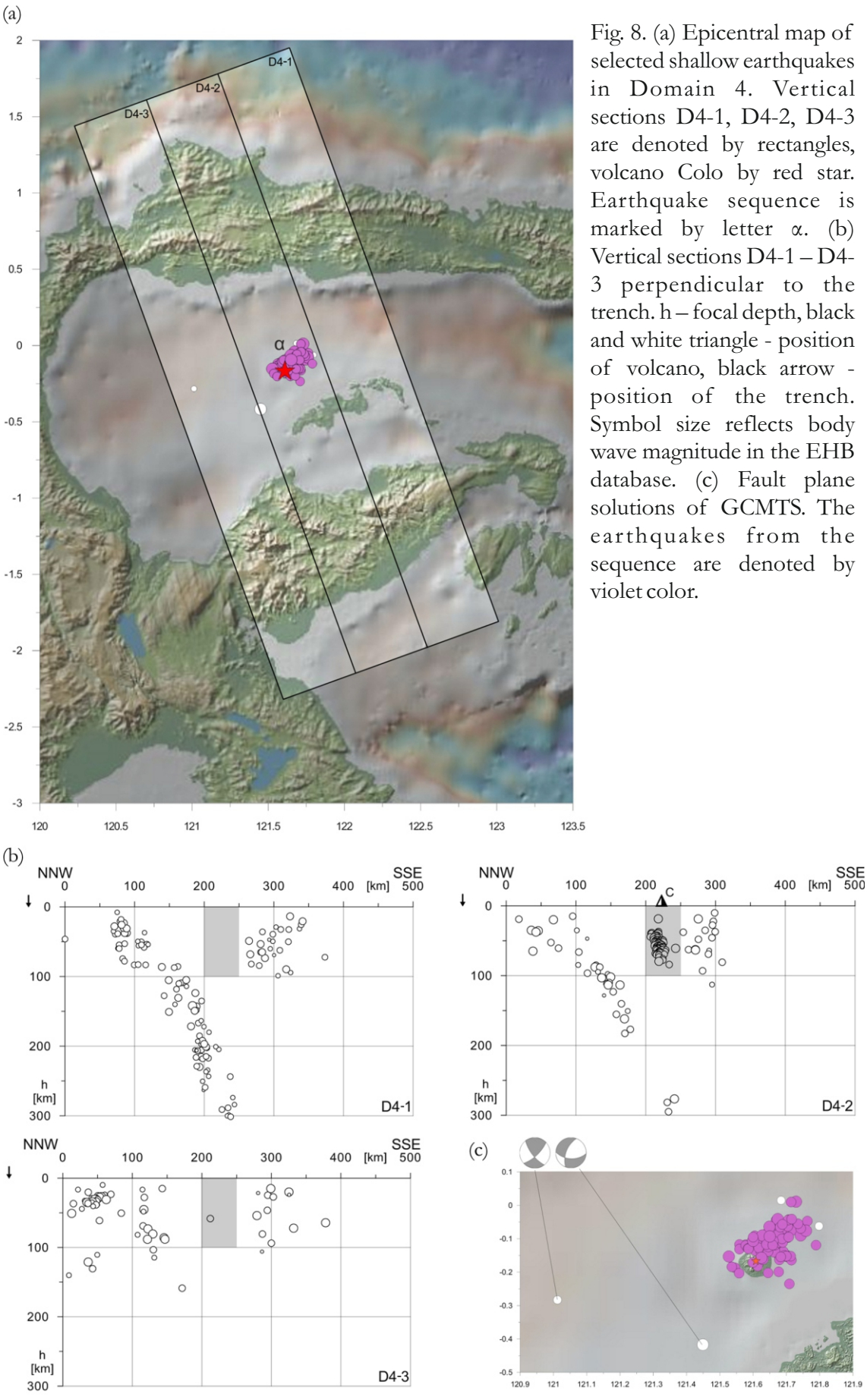

Fig. 8. (a) Epicentral map of selected shallow earthquakes in Domain 4. Vertical sections D4-1, D4-2, D4-3 are denoted by rectangles, volcano Colo by red star. Earthquake sequence is marked by letter α. (b) Vertical sections D4-1 – D4-3 perpendicular to the trench. h – focal depth, black and white triangle - position of volcano, black arrow - position of the trench. Symbol size reflects body wave magnitude in the EHB database. (c) Fault plane solutions of GCMTS. The earthquakes from the sequence are denoted by violet color.

tude range 4.5 – 5.5. As shown in the second vertical section a clear cluster of earthquake hypocenters can be delimited under the Colo volcano. The focal depth varies from the surface to 100 km. One huge earthquake sequence was found within this dataset (Fig. 6 (a), (b)).

Only two GCMTS fault plane solutions are available for earthquakes of the Colo Domain. Strike-slip movement was dominant for these earthquakes (Fig. 8 (c)).

- The 1983 sequence (Fig. 8 (a), λ)

Of 93 earthquakes of the Colo Domain 88 earthquakes occurred during 17 days. The sequence started on July 16th, 1983 when 2 events occurred and grew up to 15 events on July 19th; the last three events were recorded on August 1st. The number of events recorded by local seismic network grew during the sequence from 33 events per day on July 14th to more than 90 per day from July 18th to 21st. The major part of the huge sequence was situated at depths between 30 and 80 km beneath the Colo volcano. The magnitude varies between 4.5 and 5.4. The magnitudes are comparable during the whole sequence; therefore it can be denoted as an earthquake swarm. This sequence is associated with a large explosive eruption which started on 18 July 1983. The volcanic activity was preceded by this seismicity starting two days before the eruption. The damaging volcanic eruption continued until the end of 1983 without any further seismic activity. No GCMTS fault plane solution is available for earthquakes of this sequence (Siebert, 2002-; Venzke, 2002-).

3.5.5. Domain 5

This Domain, Manipa basin, is the only area without any active volcano recorded in The Catalogue of the Active volcanoes of the World. We decided to focus on this area because of specific earthquake sequence occurrences (Fig. 9 (a)).

- **Manipa Basin** (lat. 3.736 S; lon. 127.537 E)

The submarine Manipa basin is situated in the northern part of the Banda Sea among the islands of Buru, Seram, Ambelau and Ambon. Ninety kilometers wide, mostly submerged basin reaches 3000 m above the surrounding sea floor on average (circa 1500 m below the sea level); only several parts of this structure reach the sea level and form subaerial islands. A 2500 m high seamount is situated in the central part of this basin (Siebert, 2002-; Venzke, 2002-), see Fig. 7 (c). The major type of rocks at the islands is andesite. According

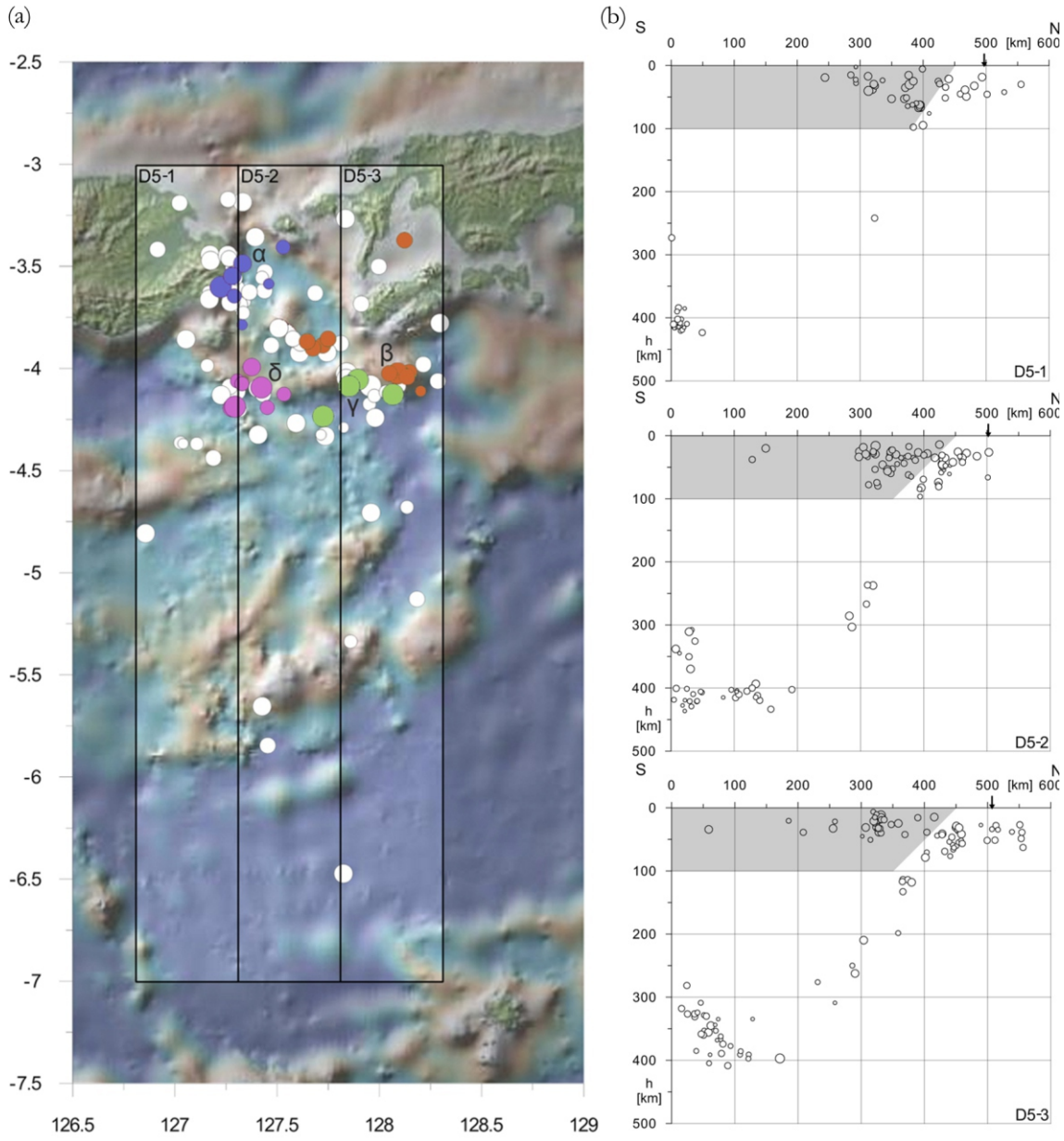

Fig. 9. (a) Epicentral map of selected shallow earthquakes in Domain 5. Vertical sections D5-1, D5-2, D5-3 are denoted by rectangles. Earthquake sequences are marked by letters α, β, γ, δ. (b) Vertical sections D5-1 – D5-3 perpendicular to the trench. h – focal depth, black arrow - position of the trench. Symbol size reflects body wave magnitude in the EHB database. (c) Profiles showing the topography of the Manipa basin area. Profiles p1, p2, p3, p4 are denoted by white lines at two basemaps. d – sea floor depth (d) Fault plane solutions of GCMTS. Bounded diagrams belong to events from earthquake clusters.

(c)

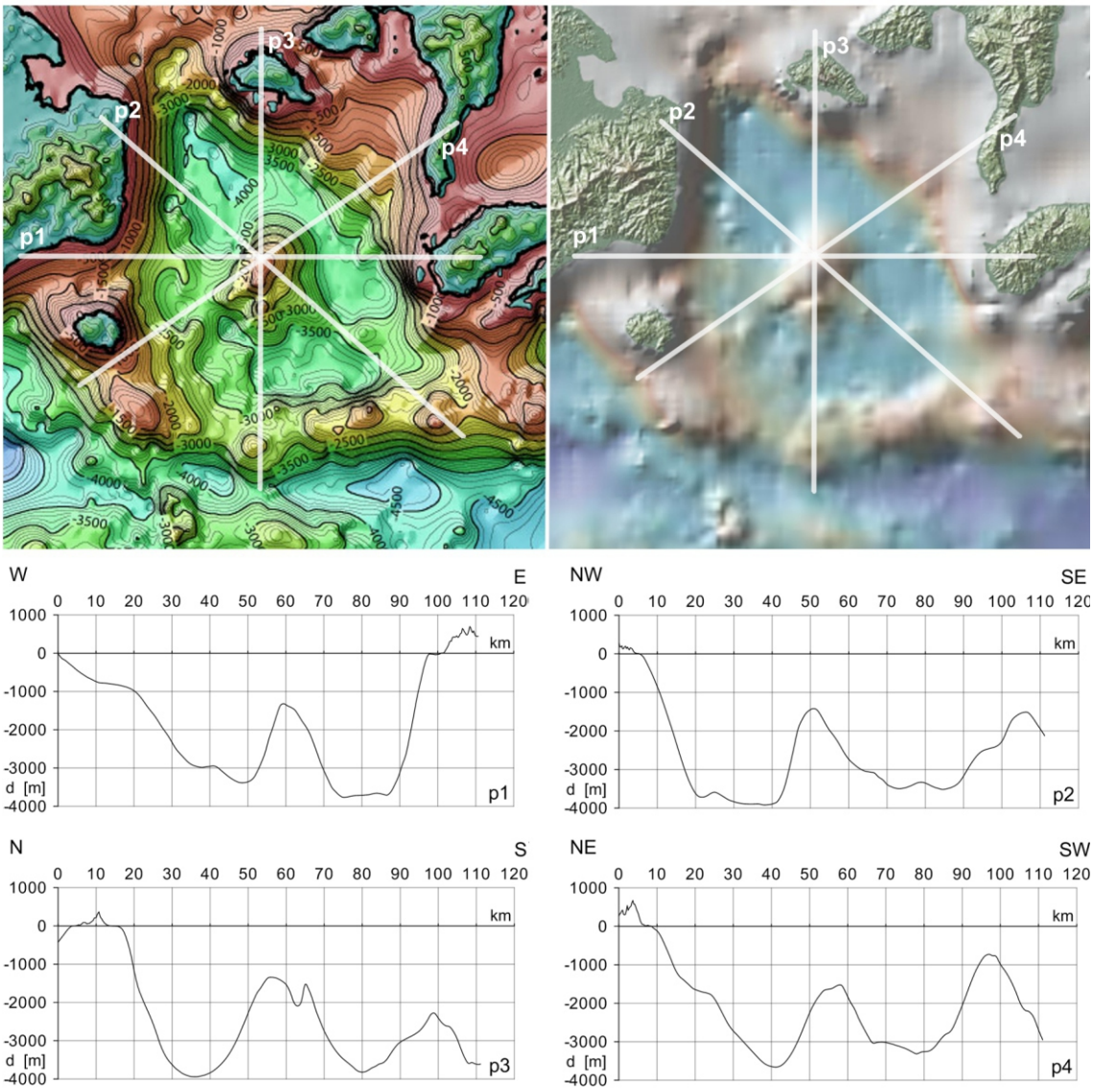
p1
p2
p3
p4
W
E
NW
SE
N
S
NE
SW
km
d [m]
0 10 20 30 40 50 60 70 80 90 100 110 120
1000
0
-1000
-2000
-3000
-4000

(d)

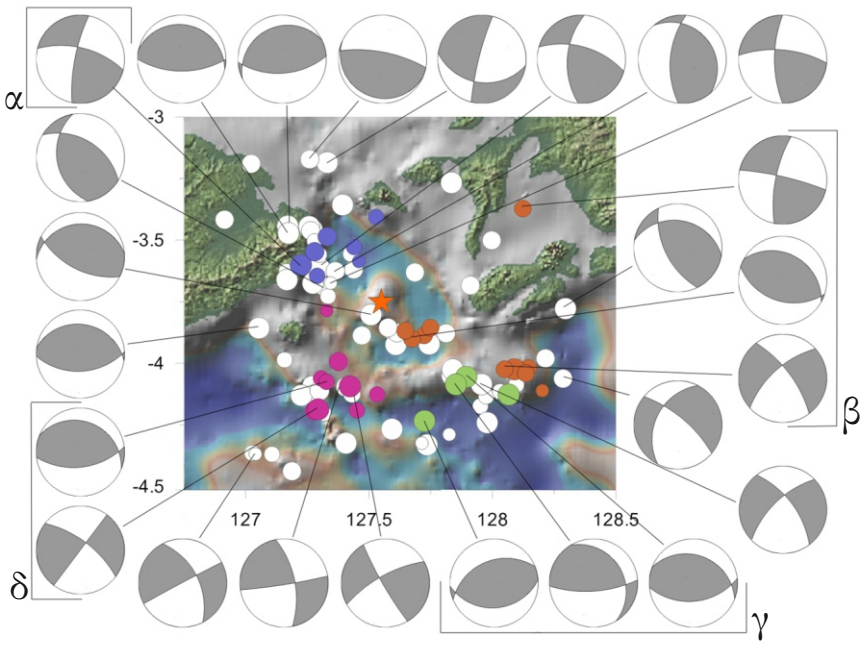
α
β
γ
δ
-3
-3.5
-4
-4.5
127
127.5
128
128.5

to a detailed geochemical analysis at the Seram Island, the samples were of high-K character, which is clearly different to lavas studied in the southern Banda Sea, where the low-K suite is lacking (Honthaas, 2008). No volcanic activity has been recorded within the basin during the observed period (Siebert, 2002-; Venzke, 2002-).

3.5.5.1. Seismicity in the domain

Three cross sections in the N- S azimuth covered the Domain 5 area. One hundred three earthquakes occurred within the overlying lithospheric wedge in the magnitude range 3.1 – 6.4. The focal depth varies from the surface to 100 km. Four huge earthquake sequences were found within this dataset (Fig. 9 (a), (b)).

The GCMTS fault plane solutions were computed for 16 events which are not within the sequences. One half of fault plane solutions was of mostly strike-slip character with some dip-slips, the second half was of mainly of thrust fault character (Fig. 9 (d)).

- The 2006 sequence (Fig. 9 (a), λ)

The sequence consists of six events that occurred during 12 days between March 14th and 25th, 2006. The focal depth was between 20 and 65 km and the magnitude range 4.4 – 6.4. The sequence was situated in the northwestern part of the Manipa Basin. Only one GCMTS fault plane solution is available; it is of strike-slip character.

- The 1997 sequence (Fig. 9 (a), β)

The sequence contains ten events. Two phases can be distinguished within the sequence; the first one started on December 26th, 1996 and lasted 12 days to January 7th, 1997 (6 events); the second one occurred during two hours on January 25th, 1997 (4 events). The focal depth varies between 15 and 40 km. The magnitude reaches from 4.7 to 5.0 with one exception of the strongest earthquake with m_b 5.8 (2nd event). Therefore, the sequence can be denoted as either seismic swarm or aftershock sequence. The two parts of the sequence also differ in their position: the first one is situated at the outer SE side of the Manipa basin slope, the second one within the basin close to the central seamount. The GCMTS fault plane solutions were calculated for three events. Two of them are dominantly of strike slip character; the third one is of thrust fault character.

- The 1983 sequence (Fig. 9 (a), γ)

The sequence consists of four events that occurred in 3 days between March 12th and 14th, 1983. The focal depth of earthquakes was between 20 and 40 km. The magnitude varies

between 5.2 and 5.9. The sequence is situated in the south-eastern part of the basin. The GCMTS fault plane solutions were calculated for three events; they are predominantly of thrust fault character.

- The 2000 sequence (Fig. 9 (a), δ)

Nine earthquakes occurred during two days between August 28th and 29th, 2000. Seven from nine events were triggered during five hours on 28 August. The focal depth was between 15 and 80 km. The magnitude varies from 4.5 to 6.4. The sequence was situated in the south-southwestern part of the basin. The GCMTS fault plane solutions were calculated for two events. One of the mechanisms was of strike-slip character, the second one of thrust fault character.

4. Conclusions

The analysis of spatial distribution of earthquake foci and of available focal mechanisms enabled us (1) to delimitate the earthquakes occurring in the overlying lithospheric wedge; (2) to study the spatial, time and magnitude dependences in this dataset; (3) to correlate it with the position of volcanoes at the surface; to determine the state of stress and to estimate the tectonic regime of the area. The results of this analyses enabled us to formulate the following conclusions:

1. The investigated volcanoes can be separated into two groups according to their position in the overall structure of the subduction zone: (a) the volcanoes that are not directly related to the active subduction. This group consists of Emperor of China, Nieuwerkerk and Gunungapi Wetar volcanoes; (b) the subduction-related volcanoes: Wurlali, Teon, Nila, Serua, Manuk, Banda Api and Colo.

The following conclusions are valid only for (b) group.

2. The earthquakes within the overlying lithospheric wedge occur preferentially in the area beneath volcanoes. The depth range of clusters of earthquakes varies around 50 km. We interpret these clusters as Seismically Active Columns. The occurrences of SAC enable us to conclude that the rock medium is capable of brittle fracture and probably is not partially melted. Therefore, the source of magma is probably below the deepest events of the cluster.

3. The earthquake sequences frequently occur in the SAC. The majority of earthquake sequences is of seismic swarm character. We assume that the trigger of this sequence seismicity is magma intrusion into a brittle structure. According to the character of earthquake sequences we assume that the structure of the overlying lithospheric wedge is highly fractured.

4. In case of the Colo volcano the correlation between the volcanic activity and earthquake sequence was observed. The beginning part of seismic sequence shortly preceded the volcanic explosion, which corresponds to the idea about triggering of seismicity by magma intrusions. No similar correlation was found for other volca-

noes. The occurrence of earthquake sequences beneath the other volcanoes we interpret in the same way, but we suppose that the magma did not reach the surface.

5. Earthquake sequences were found also beneath the submarine Manipa Basin where no historical record of volcanic activity is available. In the context of sea floor morphology and geodynamical position of the Manipa Basin related to the Wadati-Benioff zone of the Seram subduction, we consider that the basin represents a wide, recently volcanically active submarine caldera structure with a volcanic cone in the middle.

References

Bolt, B. A., 1993. Earthquake and geological discovery, W.H. Freeman and Company, USA

Condie, K. C., 1997. Plate Tectonics and Crustal Evolution. New Mexico Institute of Mining and Technology Socorro, New Mexico.

Engdahl, E. R., Van der Hilst, R., Buland, R., 1998. Global teleseismic earthquake relocation with improved travel times and procedures for depth determination, *Bull. Seism. Soc. Am.* **88**, 722-743.

Hanuš, V., Vaněk, J. and Špičák, A., 2000. Seismically active fracture zones and distribution of large accumulations of metals in the central part of Andean South America. *Mineralium Deposita*, **35**, 2-20.

Hinschberger, F., Malod, J. A., Rehault, J. P., Villeneuve, M., Royer, J. Y. and Burhanuddin, S., 2005. Late Cenozoic geodynamic evolution of eastern Indonesia. *Tectonophysics*, **404**, 91–118.

Honthaas, Ch., Maury, R. C., Priadi, B., Bellon, H. and Cotten, J., 2008. The Plio–Quaternary Ambon arc, Eastern Indonesia. *Tectonophysics*, **301**, 261–281.

International Seismological Centre, EHB Bulletin, http://www.isc.ac.uk, Internat. Seis. Cent., Thatcham, United Kingdom, 2009.

Kasahara, K., 1981. Earthquake mechanics. Cambridge University Press.

Mogi, K., 1967. Earthquakes and fractures. *Tectonophysics*, **5**, 35-55.

Neumann Van Padang, M., 1951. Catalogue of the Active Volcanoes of the World Including Solfatara Fields (1951-1967). International Assotiation of Volcanology, Rome.

Park, R. G., 1983. Foundations of Structural Geology. Blackie & Son Ltd.

Siebert, L. and Simkin, T., 2002-. Volcanoes of the World: an Illustrated Catalog of Holocene Volcanoes and their Eruptions. Smithsonian Institution, Global Volcanism Program Digital Information Series, GVP-3, (http://www.volcano.si.edu/world/).

Sigurdsson, H., Houghton, B., McNutt, S. R., Rymer, H. and Stix, J., Encyclopedia of Volcanoes, Academic Press, 1999.

Syracuse, E. M. and Abers, G. A., 2006, Global compilation of variations in slab depth beneath arc volcanoes and implications, *Geochem. Geophys. Geosyst.*, **7**.

Špičák, A., Hanuš, V. and Vaněk J., 2004. Seismicity pattern: an indicator of source region of volcanism at convergent plate margins. *Physics of the Earth and Planetary Interiors*, **141**, 303-326.

Špičák, A., Hanuš, V. and Vaněk J., 2005. Seismotectonic pattern and the source region of volcanism in the central part of Sunda Arc. *Journal of Asian Earth Sciences*, **25**, 583-600.

Špičák, A., Vaněk, J. and Hanuš, V., 2009. Volcanic plumbing system and seismically active column in the volcanic arc of the Izu-Bonin subduction zone, *Geophys. J. Intern.*, **179**, 1301-1312.

Stein, S. and Wysession M., 2003. An Introduction to Seismology, Earthquakes, and Earth Structure. Cambridge University Press.

Vaněk, J., Špičák, A. and Hanuš, V., 2000. Position of the disastrous 1999 Puebla earthquake in the seismotectonic pattern of Mexico. *Bull. Seis. Soc. Amer.*, **90**, 786-789.

Venzke, E., Wunderman, R. W., McClelland, L., Simkin, T., Luhr, J. F., Siebert, L., Mayberry, G. and Sennert, S., 2002-. Global Volcanism, 1968 to the Present. Smithsonian Institution, Global Volcanism Program Digital Information Series, GVP-4 (http://www.volcano.si.edu/reports/).

Willemann, R. J. and Storchak, D. A., 2001. Data Collection at the International Seismological Centre. *Seismological Research Letters*, **72**, 440-453.